Sphaleron transitions & CME out-of-equilibrium

Soeren Schlichting

Mark Mace, SS, Raju Venugopalan PRD93 (2016) no.7, 074036
Niklas Mueller, SS, Sayantan Sharma PRL 117 (2016) no.14, 142301
Mark Mace,Niklas Mueller, SS, Sayantan Sharma in preparation

UNIVERSITY *of* WASHINGTON

Chiral magnetic effect

Discovery of new kind of conductivity for systems
with chiral fermions and chirality imbalanced

(Fukushima, Kharzeev, Warringa PRD 78 (2008) 074033)

$$\vec{j}_V \propto n_5 \vec{B}$$

n_5: axial charge imbalance
B: magnetic field

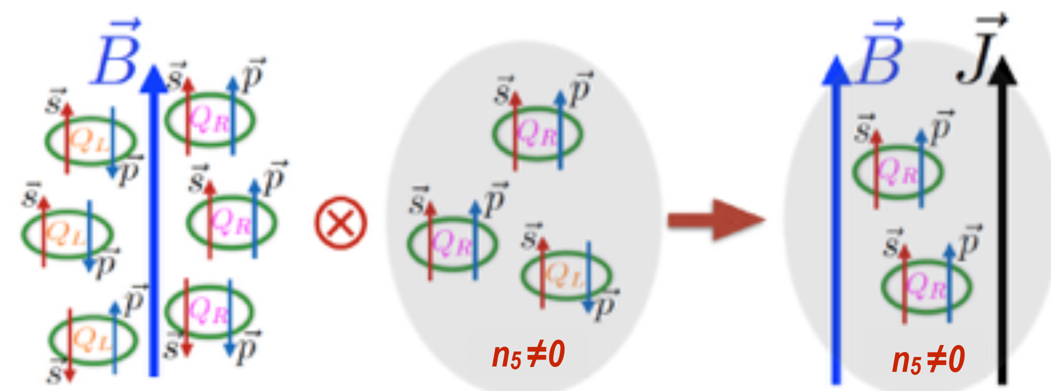

Kharzeev, Liao, Voloshin, Wang
Prog. Part. Nucl. Phys. 88 (2016) 1-28

Quantitative theoretical understanding of anomaly induced transport phenomena (CME,…) in heavy-ion collisions requires knowledge of the space-time dependence

distribution of axial charges magnetic field

Magnetic field in HIC

Spectators in off-central collisions create a strong magnetic field $eB \sim m_\pi^2$ (unit conversion $m_\pi^2 \sim 10^{14}$ T)

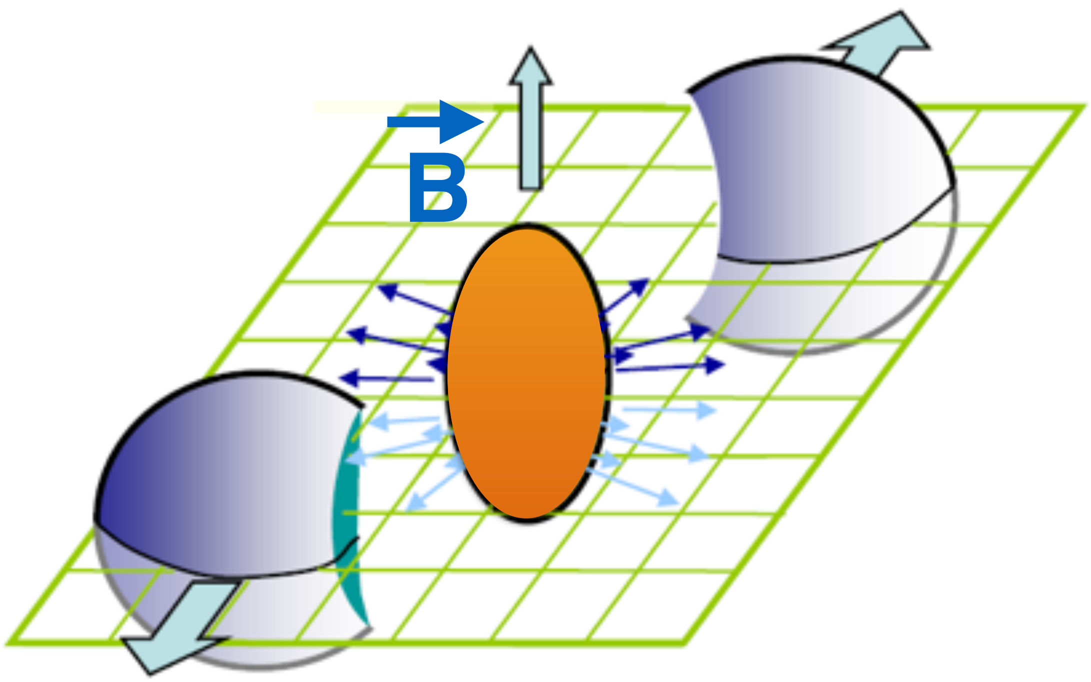

STAR PRC 81 (2010) 054908

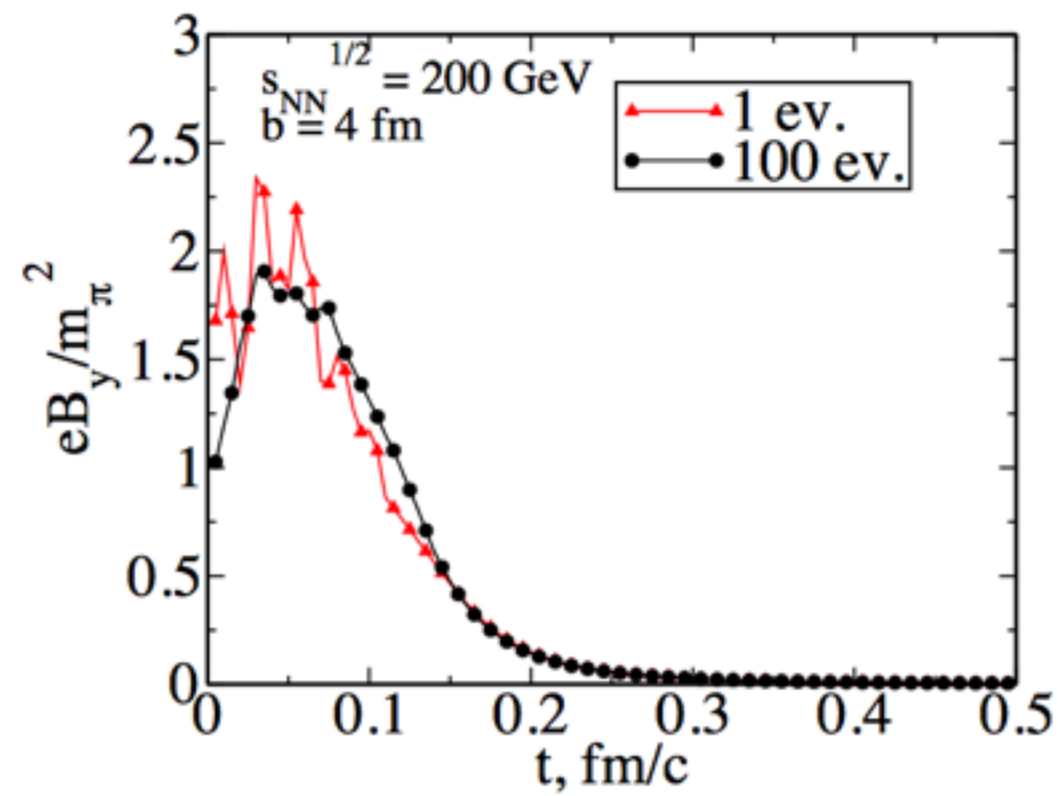

Skokov,Illarionov,Toneev
Int.J.Mod.Phys. A24 (2009) 5925-5932

However, life-time of magnetic field in vacuum is short < 1 fm/c

Significant fraction of effect should take place during the pre-equilibrium stage

Axial charge in HIC

Sourced by fluctuations of the non-abelian field strength tensor due to the axial anomaly

$$\partial_\mu j^\mu_{5,f} = 2m_f \bar{q}\gamma_5 q - \frac{g^2}{16\pi^2} F^a_{\mu\nu}\tilde{F}^{\mu\nu}_a$$

axial current $j^\mu_5 = (n_5, \vec{j}_5)$

quark mass

field-strength fluctuations $\propto \vec{E}\cdot\vec{B}$

While axial charge $\langle n_5 \rangle = 0$ naturally expects space-time dependent fluctuations of $n_5(x,t)$ in each event

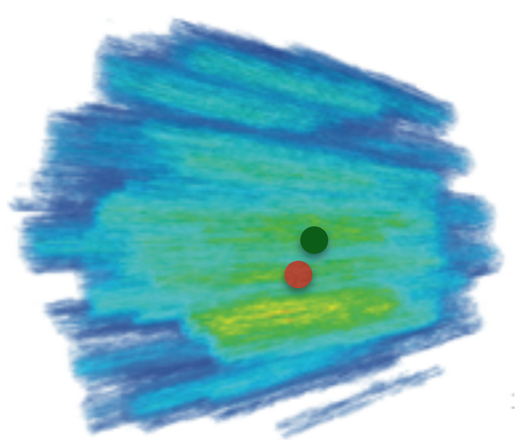

initial quark production

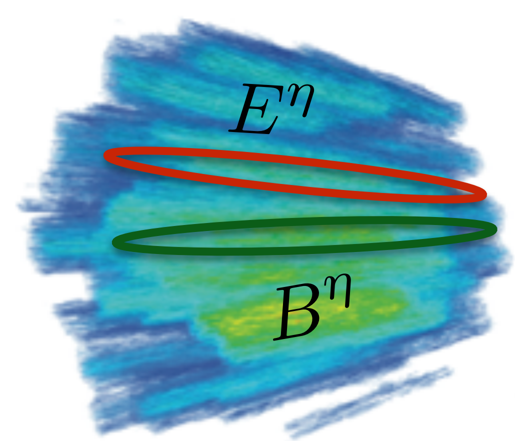

color flux tubes

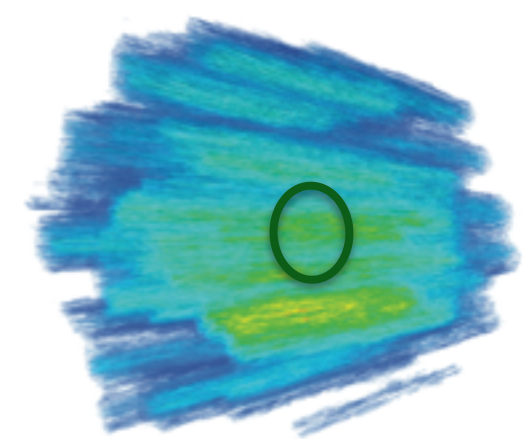

sphaleron transitions

Caveat: Since axial charge is not conserved can also decrease $n_5(x,t)$

Challenges for CME in heavy-ion collisions

... Concerning the quantitative understanding of the CME in heavy-ion collisions, the dominant theoretical uncertainties originate from

A) the initial distribution of axial charges,

B) the evolution of the magnetic field,

C) the dynamics of the CME during the pre-equilibrium stage,

D) the uncertainties in the hadronic phase and the freeze-out.

``Chiral Magnetic Effect Task Force Report,'' arXiv:1608.00982 [nucl-th]

Early time dynamics is key to overcome the challenges A), B) & C)

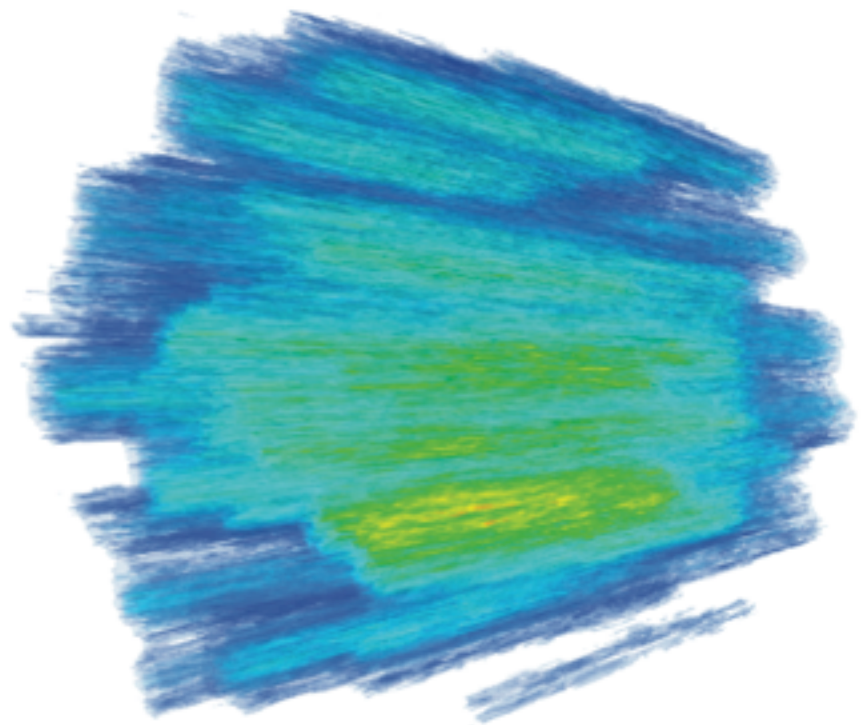 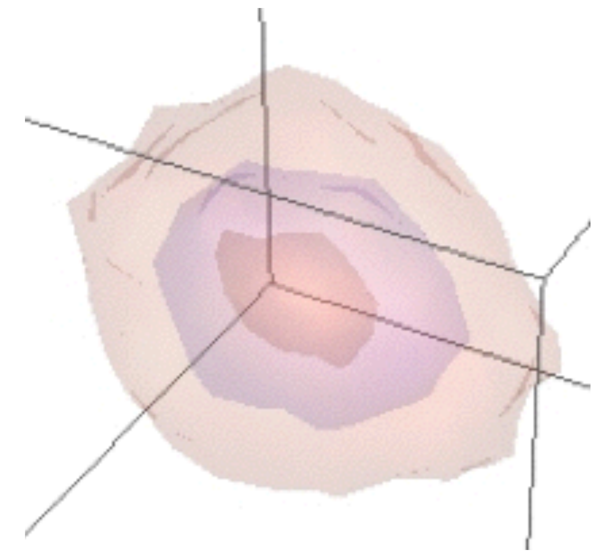

Early time dynamics and sphaleron transitions out-of-equilibrium

Early stages of HIC

Qualitatively complete picture of equilibration mechanism at weak coupling

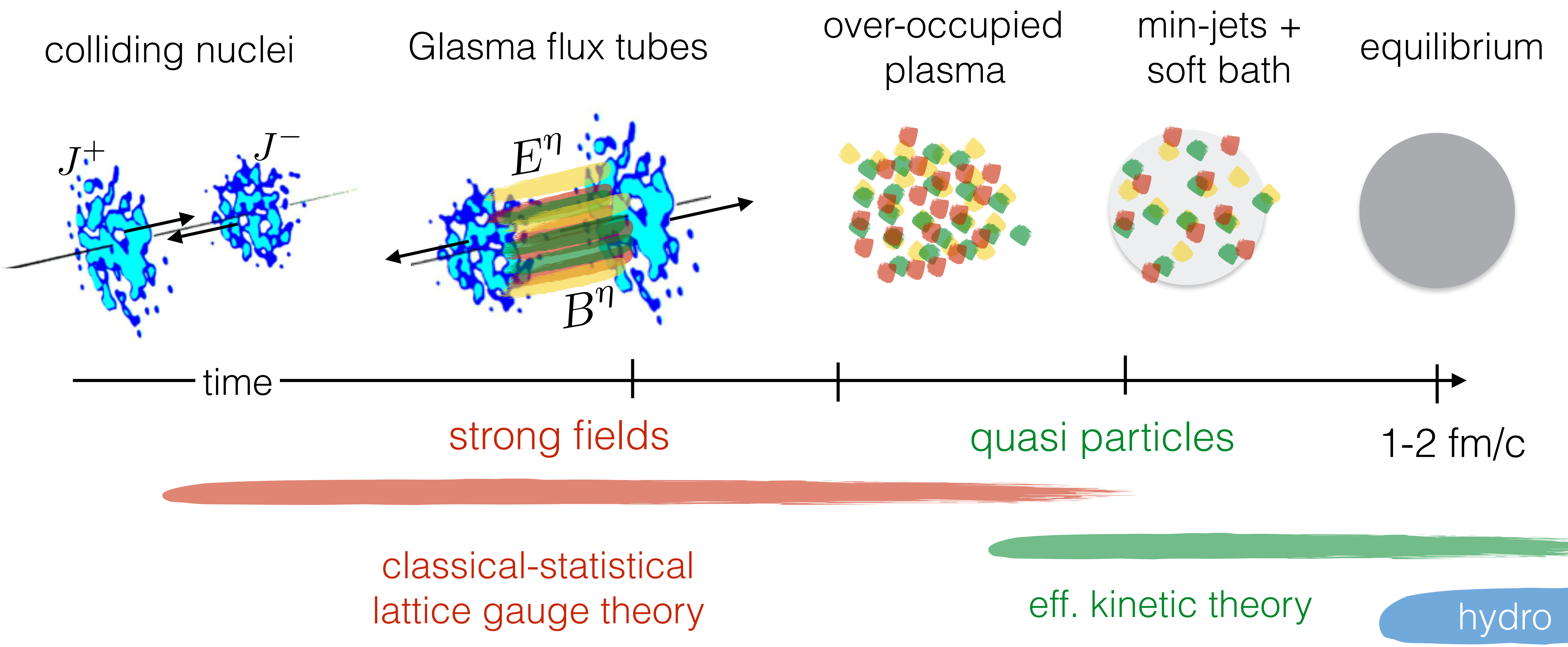

So far focus has been on dynamics of hard modes (mini-jets)

-> needs to be extended to soft modes to study axial charge production

Classical Yang-Mills dynamics & lattice topology

Early time dynamics described by classical Yang-Mills dynamics of non-perturbatively large gluon fields $f(p \sim Q_s) \sim 1/\alpha_s$

Can compute axial charge production by extracting Chern-Simons number N_{CS}

$$\frac{dN_{CS}}{dt} = \frac{g^2}{8\pi^2} \int d^3x \; E_i^a(\mathbf{x}) B_i^a(\mathbf{x})$$

By use of cooling techniques one can disentangle short range fluctuations from topological transitions

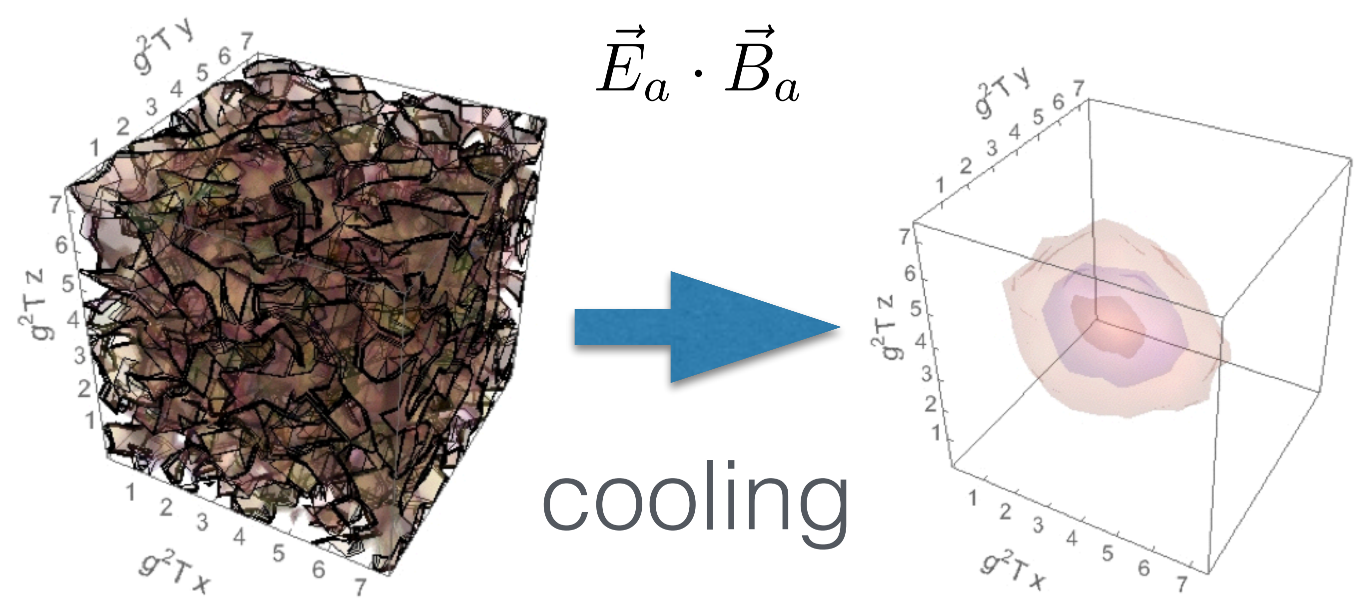

Disclaimer: So far first qualitative study neglecting long. expansion

Sphaleron transitions in the Glasma

Evolution of the Chern-Simons number for a single configuration

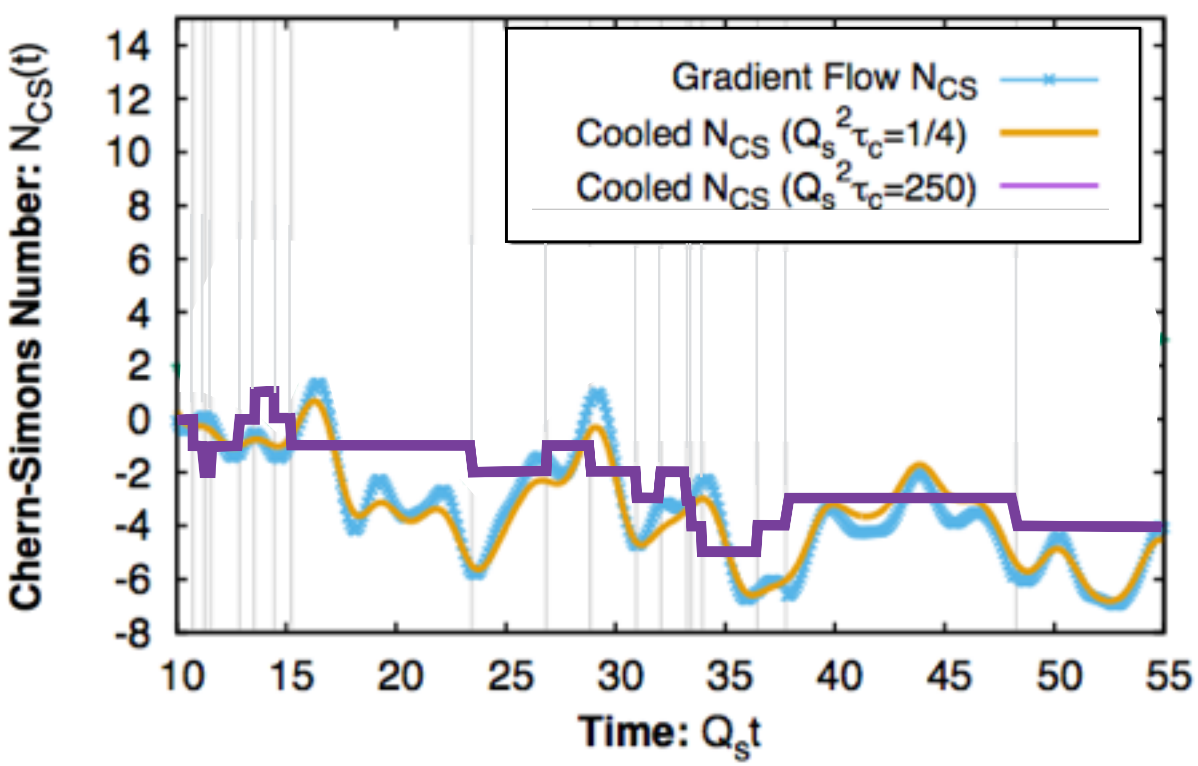

Histograms of Chern-Simons numbers

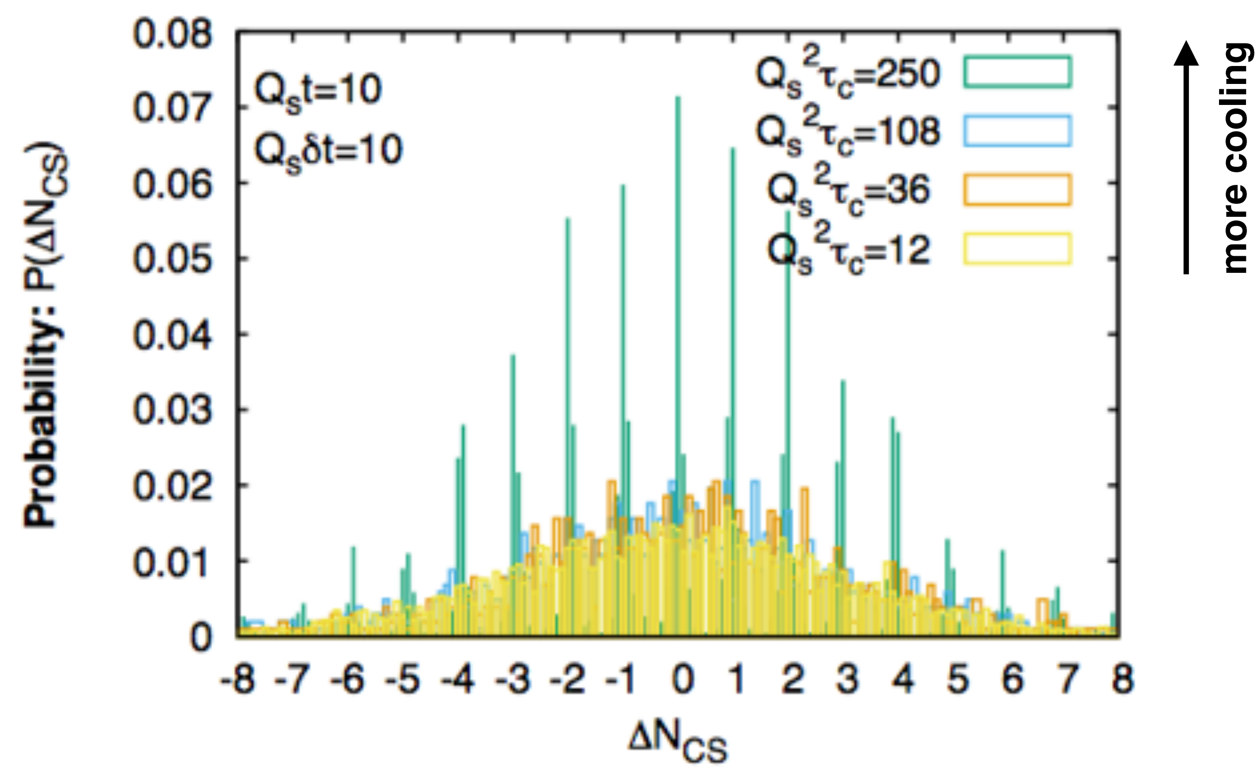

Significant number of sphaleron transitions on time scales on time scales of a few $1/Q_s$

Mace, SS, Venugopalan PRD93 (2016) no.7, 074036

Quantifying the sphaleron rate

Strong time dependence of sphaleron transition rate

-> early times dominate generation of axial charge imbalance

Sizable contribution from topologically trivial local fluctuations of field strength

Non-equilibrium sphaleron rate

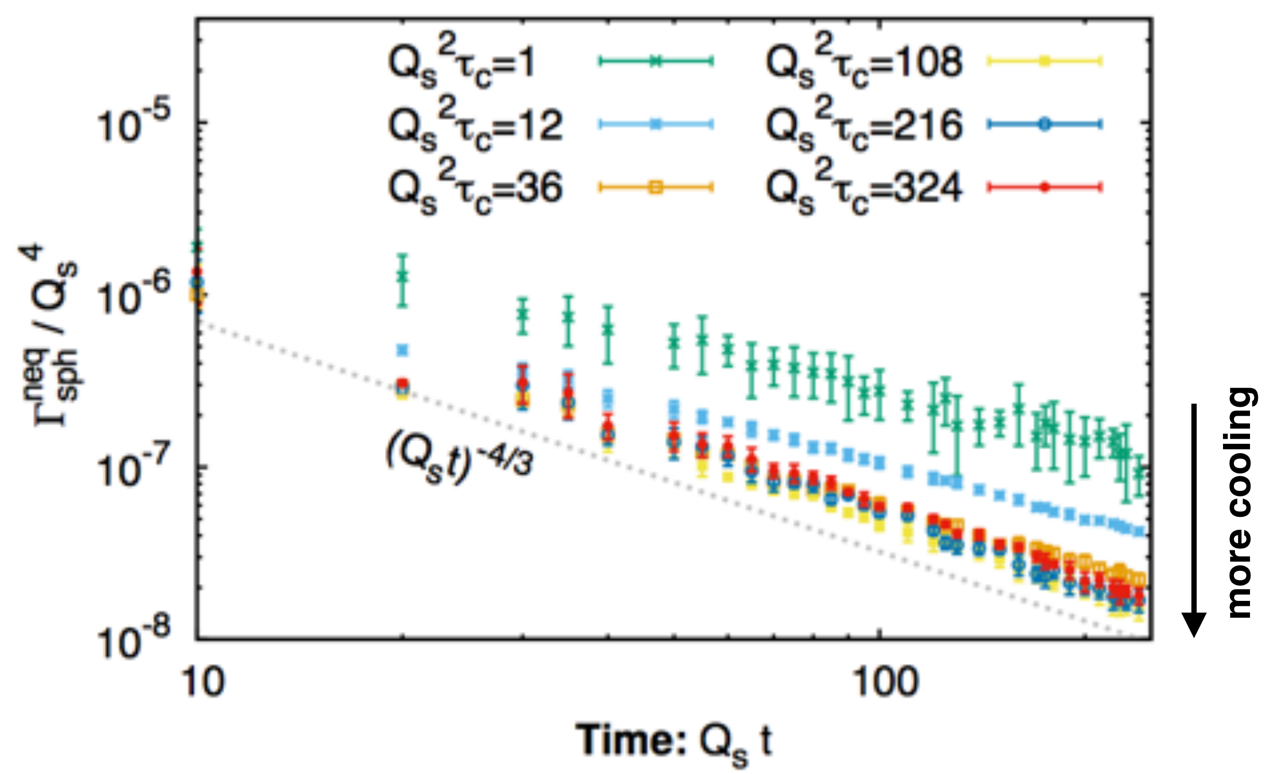

Future prospects:

Expect qualitatively similar features when extending to long. expanding relevant to HIC

Quantitative study still case requires progress in understanding longitudinal structure of initial state

Mace, SS, Venugopalan PRD93 (2016) no.7, 074036

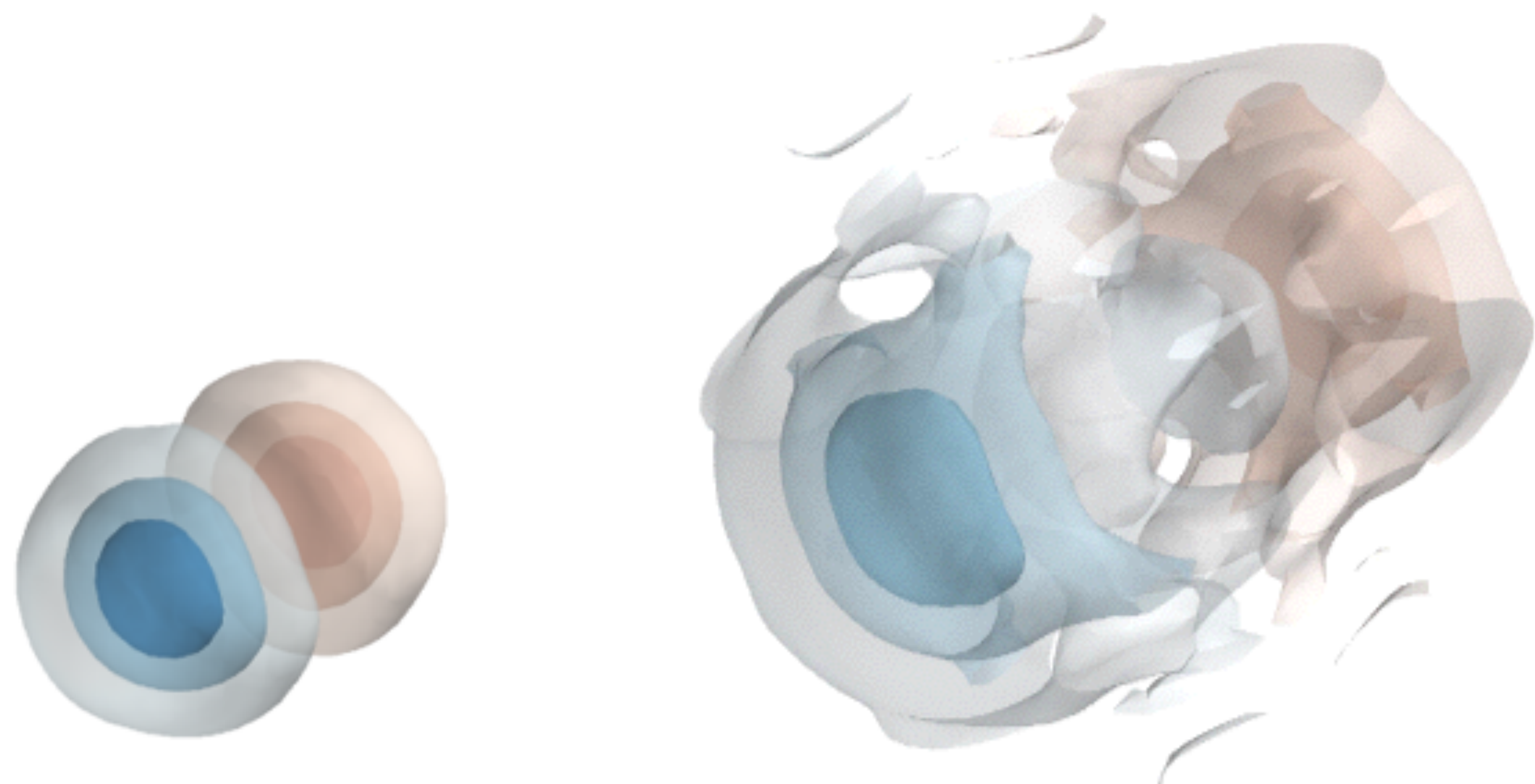

Chiral magnetic effect
& anomaly induced transport
from real-time lattice simulations

Non-equilibrium dynamics with fermions

Significant progress in understanding non-equilibrium dynamics of gluon fields

-> next step is to include fermions into non-equilibrium description

Expand the fermion field in operator basis at initial time

$$\hat{\psi}(x,t) = \sum_{p,\lambda} \hat{b}_{p,\lambda}(t=0)\phi_u^{p,\lambda}(x,t) + \hat{d}^{\dagger}_{p,\lambda}(t=0)\phi_v^{p,\lambda}(x,t)$$

and evolves the wave-functions by solving the Dirac equation

$$(i\not{D}_w - m)\hat{\psi} = 0$$

$\not{D}_w$ coupling to QCD +QED fields

measure operator expectation values $j^{\mu}_{V} = e\,\langle \hat{\bar{\psi}}(x)\gamma^{\mu}\hat{\psi}(x)\rangle$

Straightforward to include back reaction to gauge sector $D_{\mu}F^{\mu\nu} = j^{\nu}$

Disclaimer: Development of this is in progress will present first results in a clean theoretical setup: single sphaleron transition + magnetic fields

Axial anomaly in real-time

Non-trivial realization of axial anomaly for Wilson fermions which requires decoupling of fermion doublers

Karsten, Smit Nucl. Phys. B183 (1981) 103

$$\partial_\mu j_5^\mu(x) = 2m < \bar{\psi}(x) i\gamma_5 \psi(x) > + r_W < W(x) > \rightarrow -\frac{g^2}{8\pi^2} \mathrm{Tr} F_{\mu\nu} F^{\mu\nu}$$

Cross-check anomaly with improved Wilson and overlap fermions

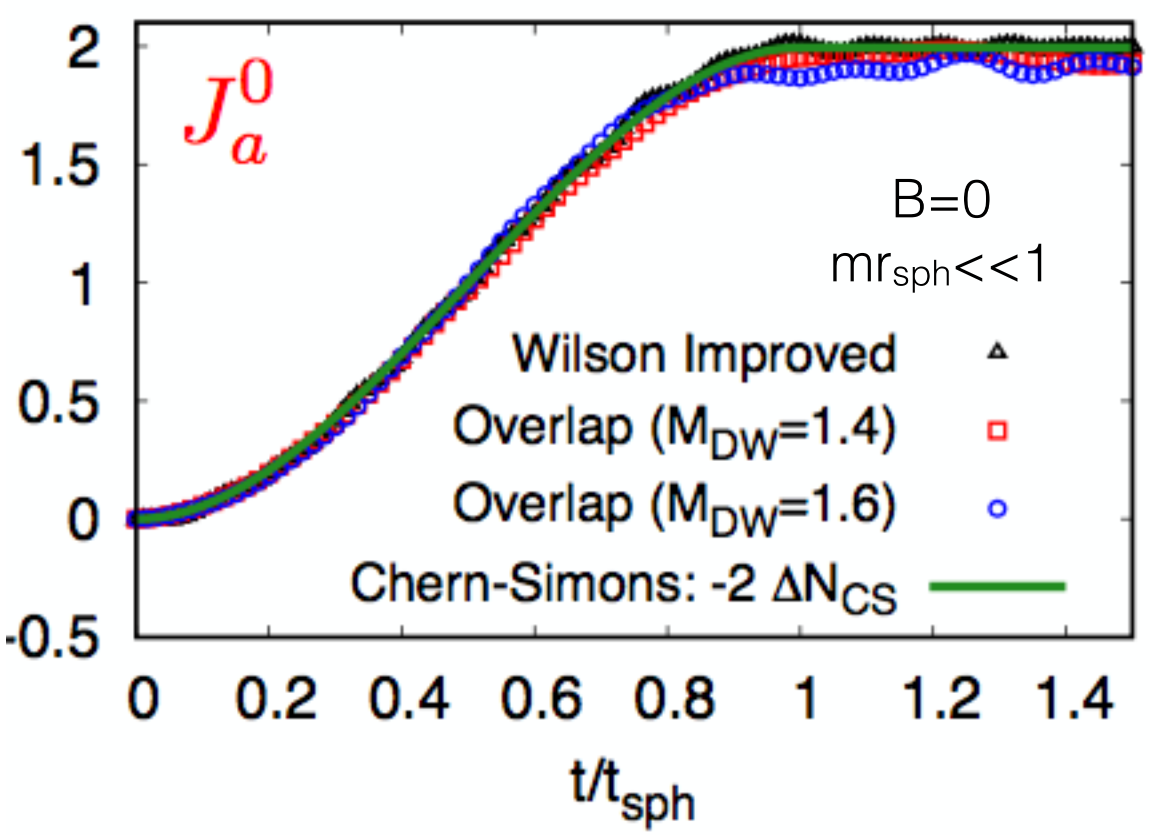

Sphaleron transition leads to a unit change of Chern-Simons number

$$\Delta N_{CS} = \frac{g^2}{8\pi^2} \int d^4x \ \vec{E}_a \vec{B}_a$$

an induces an imbalance of axial charge

$$\Delta J_5^0 = -2\Delta N_{CS} + 2m_f \int d^4x \langle \bar{\psi} i\gamma_5 \psi \rangle$$

(M.Mace,N.Mueller,SS, S. Sharma in preparation)

Spectral properties

Microscopic picture:

Extract fermion spectrum by projection of gauge invariant two-point correlation function onto free fermion states

$$n_h^u(p) = \int u_p^{(h)} \langle \psi^\dagger(x) U_{xy} \psi(y) \rangle u_p^{\dagger(h)} \; e^{-ip(x-y)}$$

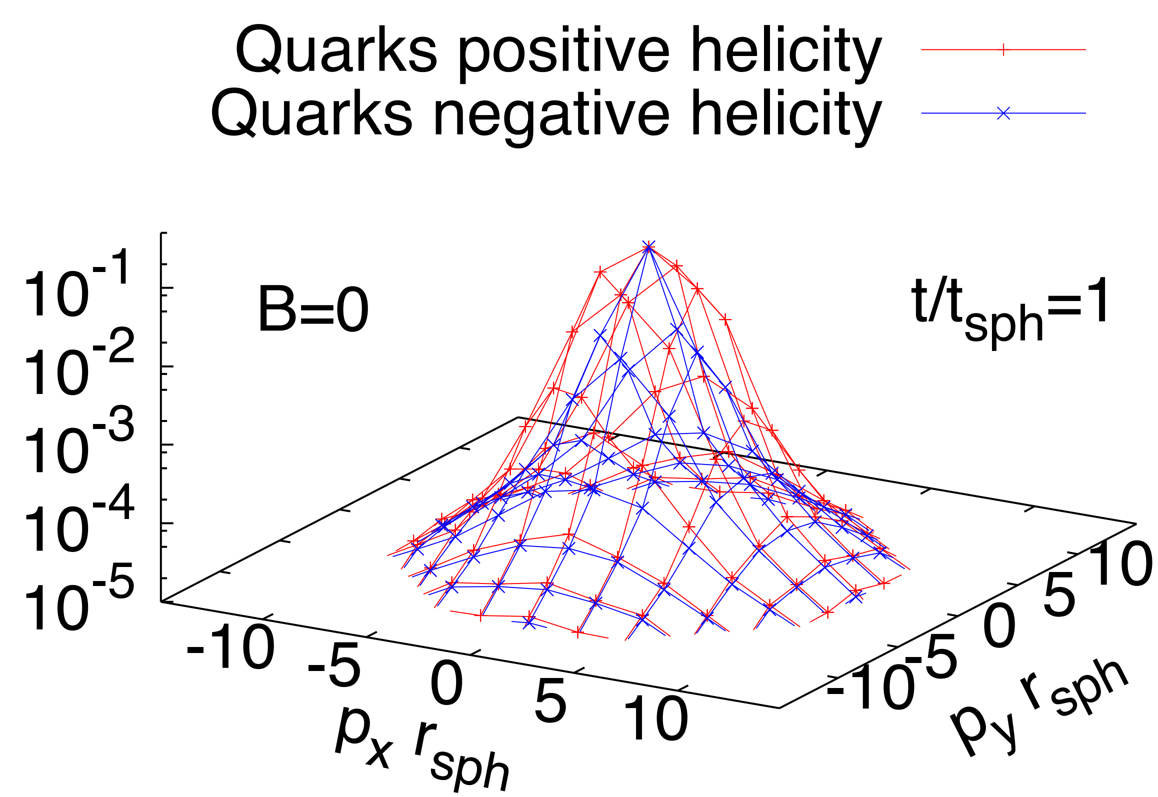

Sphaleron transition leads to production of soft fermions with an excess of positive over negative helicity

(M.Mace, N.Mueller, SS, S. Sharma in preparation)

CME Dynamics

Sphaleron transition induces local imbalance
of axial charge density j_5^0

Axial charge j_5^0 Vector current j_V^z Vector charge j_V^0

Non-zero magnetic field B_z -> vector current j_V^z is generated

Vector current j_V^z leads to separation of electric charges j_V^0
along the B-field direction

(N.Mueller, SS, S. Sharma PRL 117 (2016) no.14, 142301)

CME Dynamics

Sphaleron transition induces local imbalance
of axial charge density j_5^0

Axial charge j_5^0

Vector current j_V^z

Vector charge j_V^0

Non-zero magnetic field B_z -> vector current j_V^z is generated

Vector current j_V^z leads to separation of electric charges j_V^0
along the B-field direction

(N.Mueller, SS, S. Sharma PRL 117 (2016) no.14, 142301)

CME Dynamics

Sphaleron transition induces local imbalance
of axial charge density j_5^0

Axial charge j_5^0 | Vector current j_V^z | Vector charge j_V^0

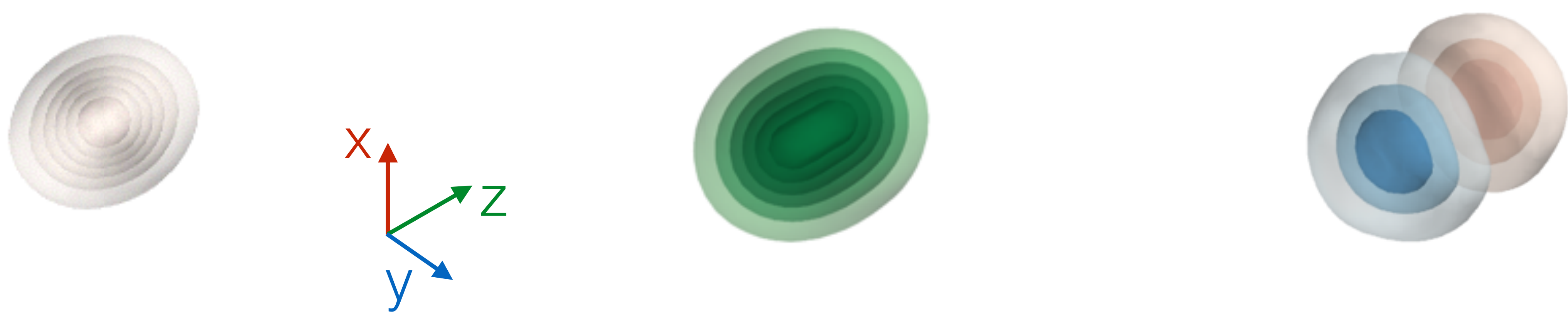

Non-zero magnetic field B_z -> vector current j_V^z is generated

Vector current j_V^z leads to separation of electric charges j_V^0
along the B-field direction

(N.Mueller, SS, S. Sharma PRL 117 (2016) no.14, 142301)

CMW Dynamics

Vector charge imbalance j_V^0 generates an axial current j_5^z
so that axial charge also flows along the B-field direction

Axial charge j_5^0 | Vector current j_V^z | Vector charge j_V^0

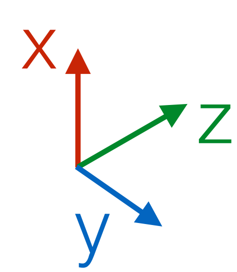

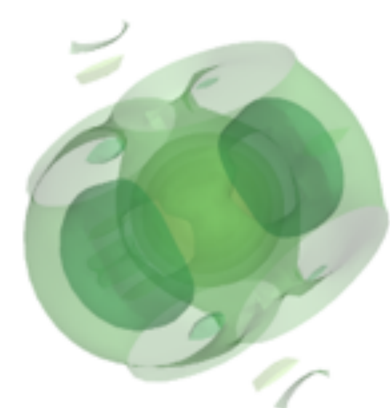

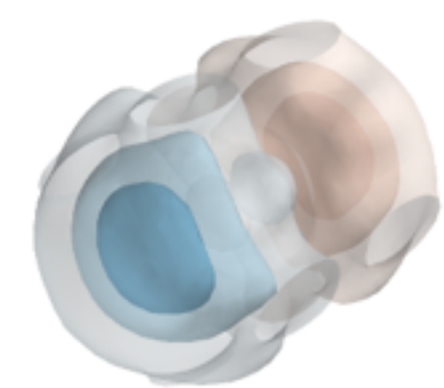

Shock-wave of vector charge and axial charge
propagating along B-field direction

(N.Mueller, SS, S. Sharma PRL 117 (2016) no.14, 142301)

CMW Dynamics

Vector charge imbalance j_V^0 generates an axial current j_5^z
so that axial charge also flows along the B-field direction

Axial charge j_5^0 Vector current j_V^z Vector charge j_V^0

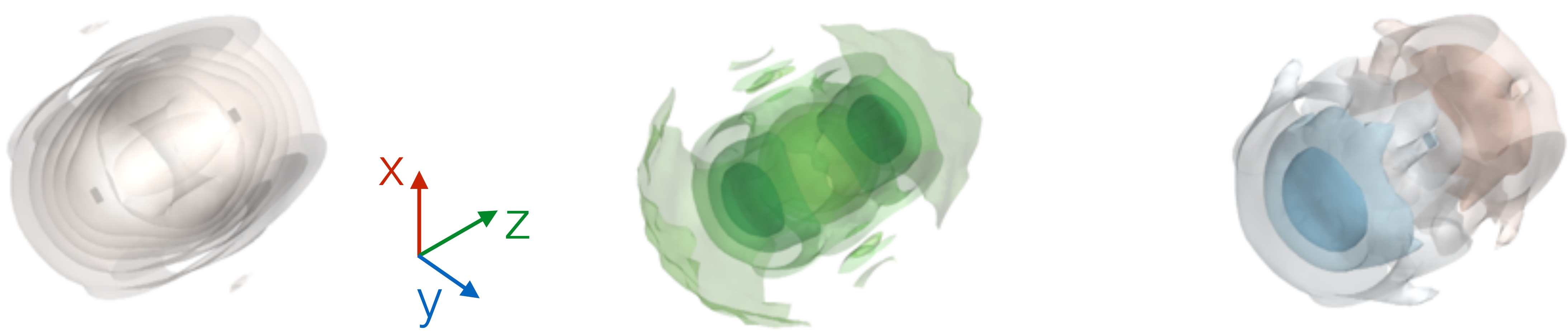

Shock-wave of vector charge and axial charge
propagating along B-field direction

(N.Mueller, SS, S. Sharma PRL 117 (2016) no.14, 142301)

CMW Dynamics

Vector charge imbalance j_V^0 generates an axial current j_5^z
so that axial charge also flows along the B-field direction

Axial charge j_5^0 | Vector current j_V^z | Vector charge j_V^0

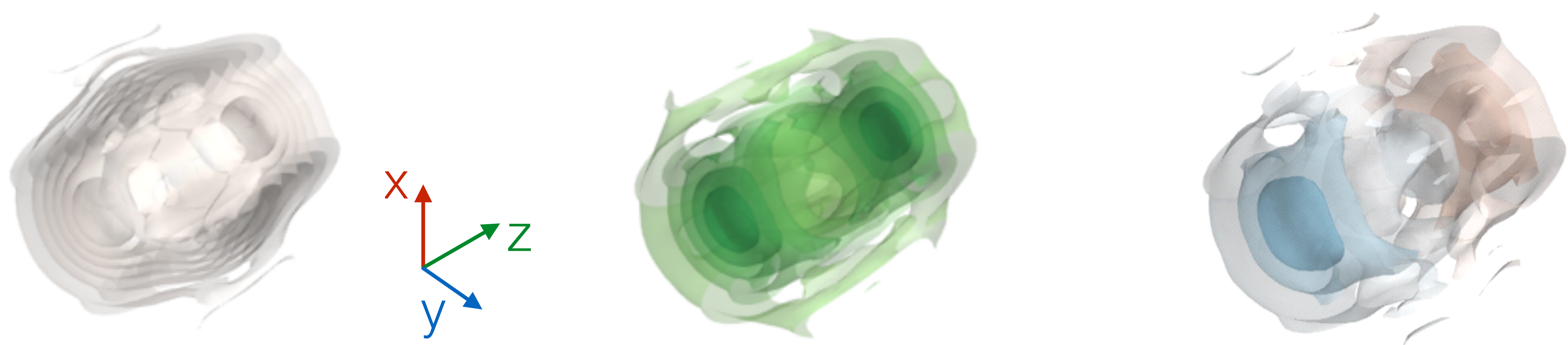

Shock-wave of vector charge and axial charge
propagating along B-field direction

(N.Mueller, SS, S. Sharma PRL 117 (2016) no.14, 142301)

Non-equilibrium CME dynamics

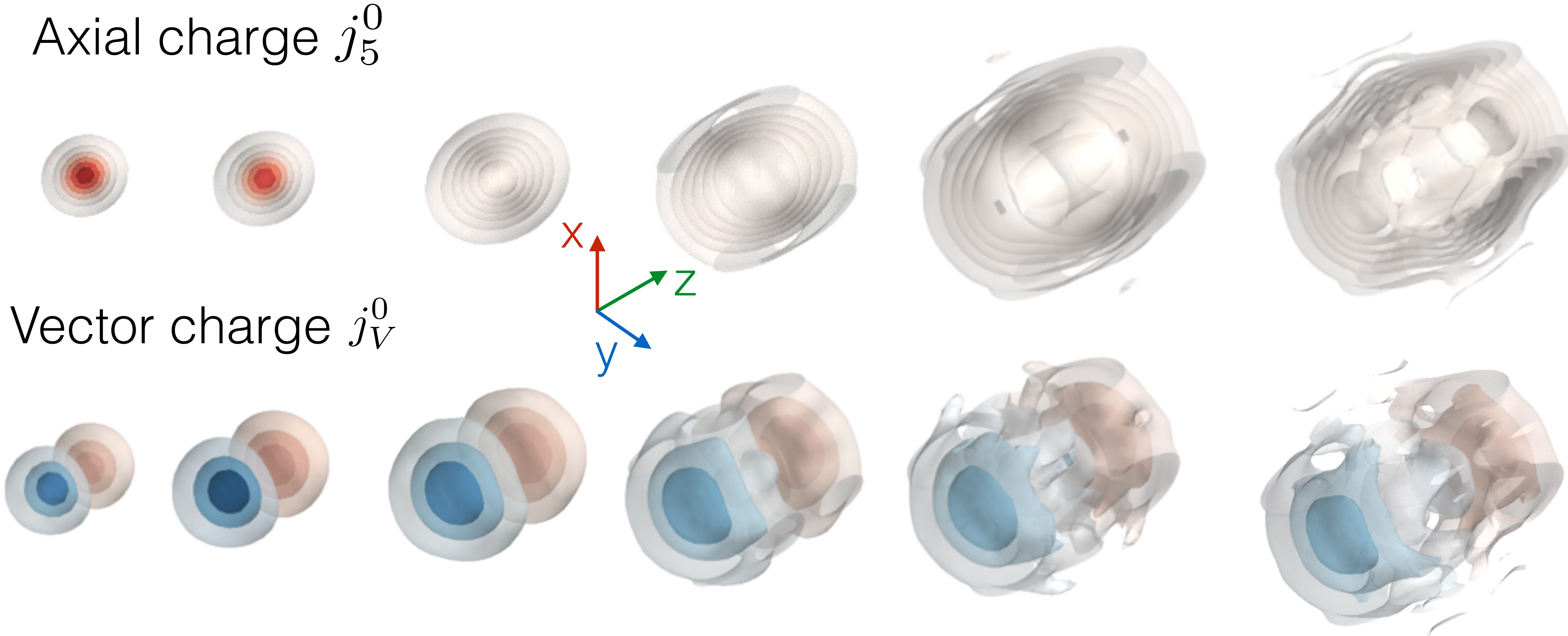

Clear separation of electric charge j_V^0 along the B-field direction

Proof of principle of a microscopic description of anomalous transport phenomena out-of-equilibrium

(N.Mueller, SS, S. Sharma PRL 117 (2016) no.14, 142301)

Quark mass dependence

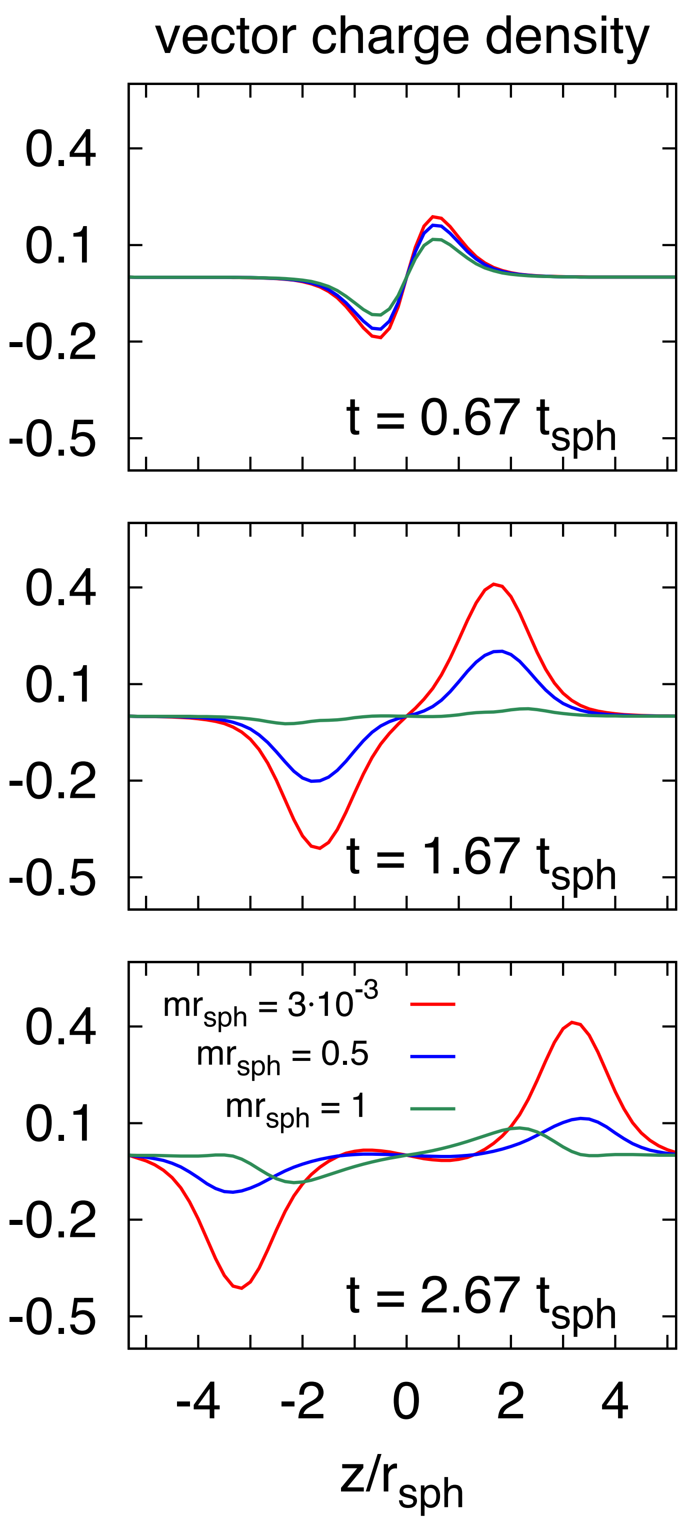

Light quarks (mr_{sph}<<1)

Chiral magnetic wave leads to non-dissipative transport of axial and vector charges

Evolution at late times well described by anomalous hydrodynamics

Heavy quarks (mr_{sph}~1)

Dissipation of axial charge leads to significant reduction of axial charge density already for $mr_{sph}\sim 1$

How to include dissipative effects into macroscopic description?

(M.Mace, N.Mueller, SS, S. Sharma in preparation)

Conclusions & Outlook

First calculations of axial charge production based on weakly coupled pre-equilibrium dynamics

Sphaleron transition rate enhanced during the early stages of HIC

Still need to quantify different sources of $n_5(x,t)$ in realistic environment

Development of real-time lattice techniques to study pre-equilibrium dynamics of fermions

Successful microscopic description of anomalous transport phenomena in rather simplistic setup

Next step will be to study quark production and axial charge production for realistic gauge field configurations

Ultimate goal to provide constraints on initial conditions for anomalous hydrodynamics should be within reach

Extend simulations to include back-reaction on electro-magnetic fields

Constraints on the extension of the life-time of magnetic field

Backup

Early times ($0 < Q_S\tau < 1$)

Strong boost invariant classical fields E^η, B^η created immediately after the collision

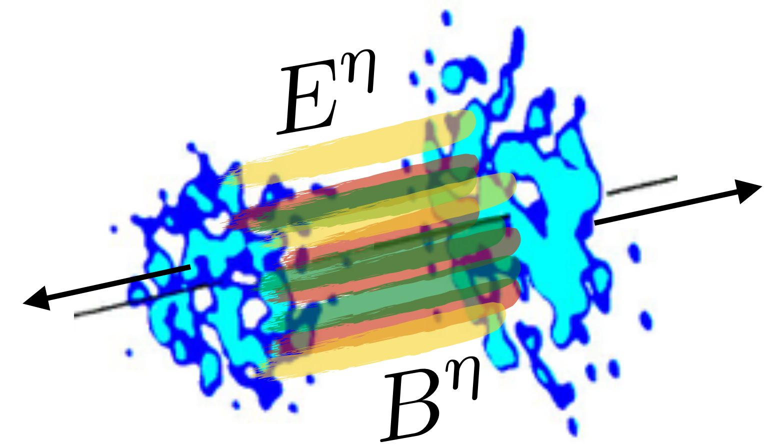

Decoherence of classical fields occurs on a time scale $1/Q_S$

- next-to-leading order (α_s) corrections break boost invariance

  -> plasma instabilities lead to an increase of longitudinal pressure

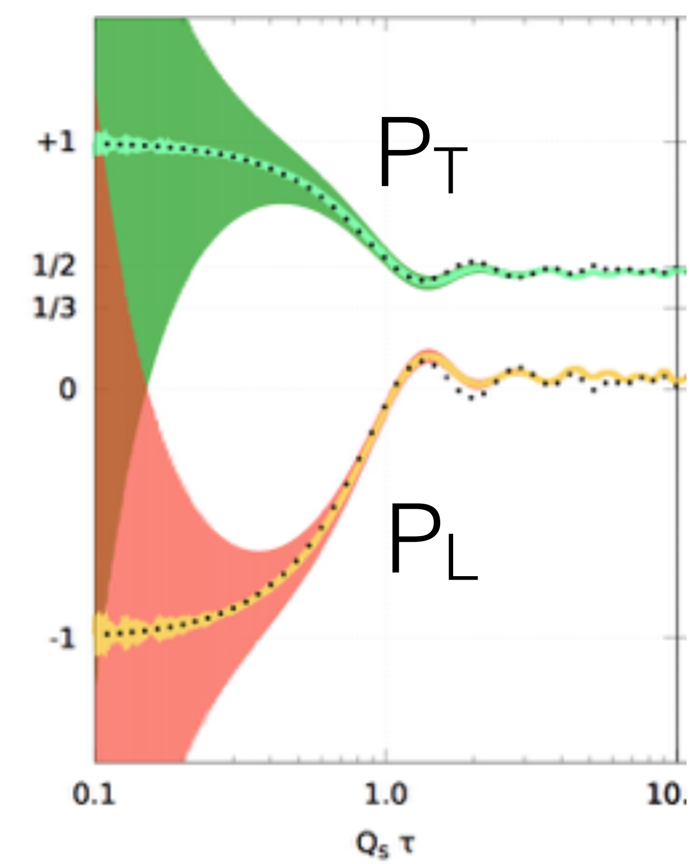

(Epelbaum,Gelis PRL 111 (2013) 232301,
Berges, Schenke, SS , Venugopalan NPA 931 (2014) 348-353)

Classical regime ($1<Q_S\tau<\alpha_S^{-3/2}$)

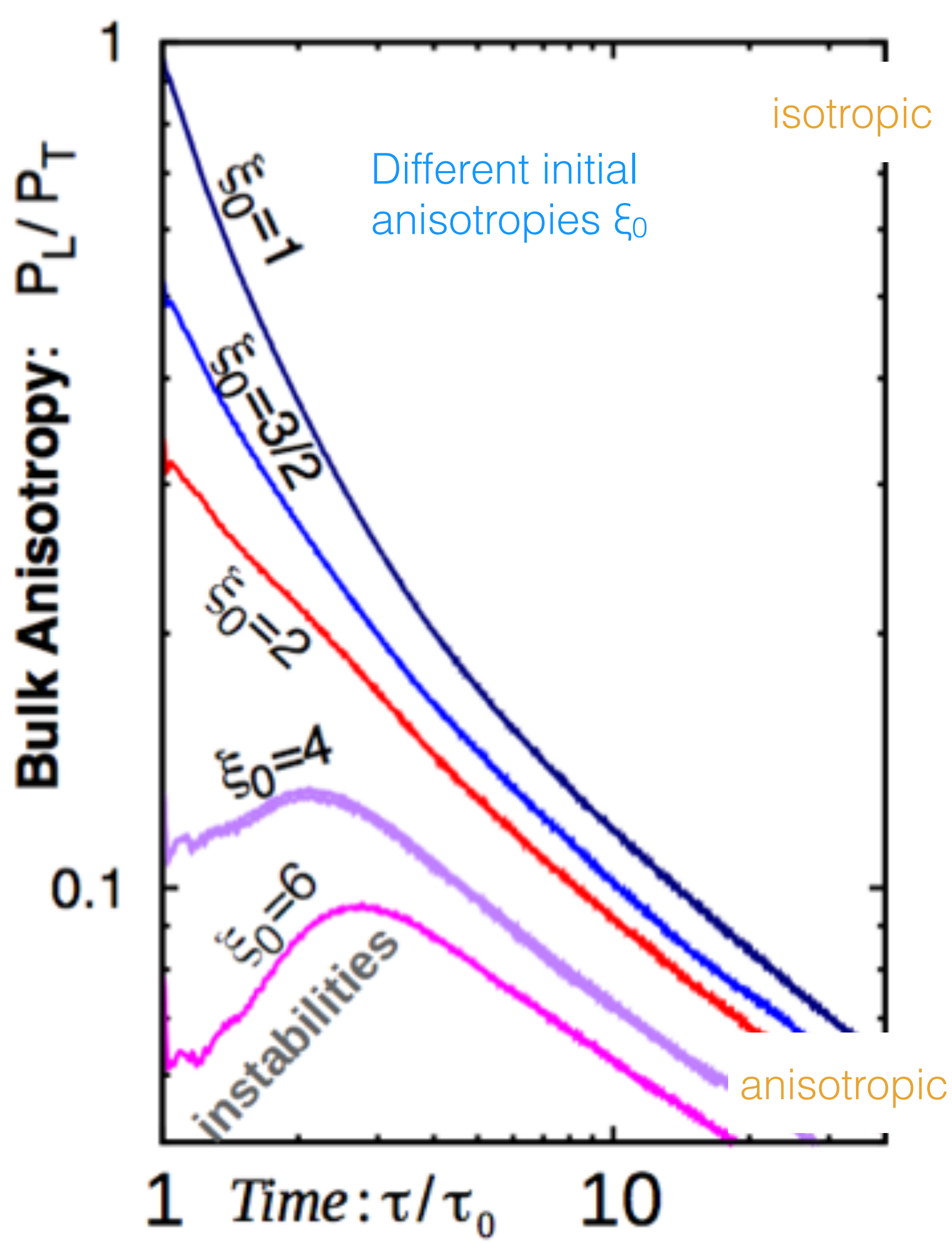

Classical field interactions are not sufficiently strong to restore isotropy beyond $1/Q_S$

-> anisotropy of the plasma increases again

No sign of plasma instabilities playing a significant role at later times $Q_S\tau>1$

(Berges, Boguslavski, SS, Venugopalan PRD 89 (2014) 074011; 89 (2014) 114007)

Classical regime ($1<Q_s\tau<\alpha_s^{-3/2}$)

Classical field evolution ($\tau>1/Q_s$) of hard modes can be accurately described in terms of weakly interacting quasi particles

-> classical particle/field duality

Effective kinetic description

(Arnold, Morre, Yaffe JHEP 0301 (2003) 030)

$$\frac{df}{dt} = -C_{2\leftrightarrow 2}[f] - C_{1\leftrightarrow 2}[f]$$

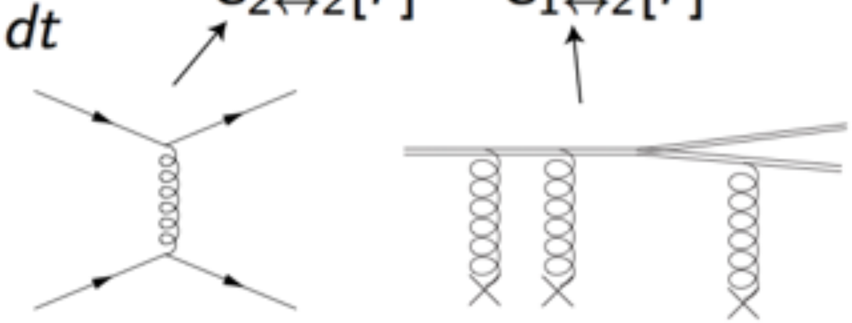

Kinetic theory

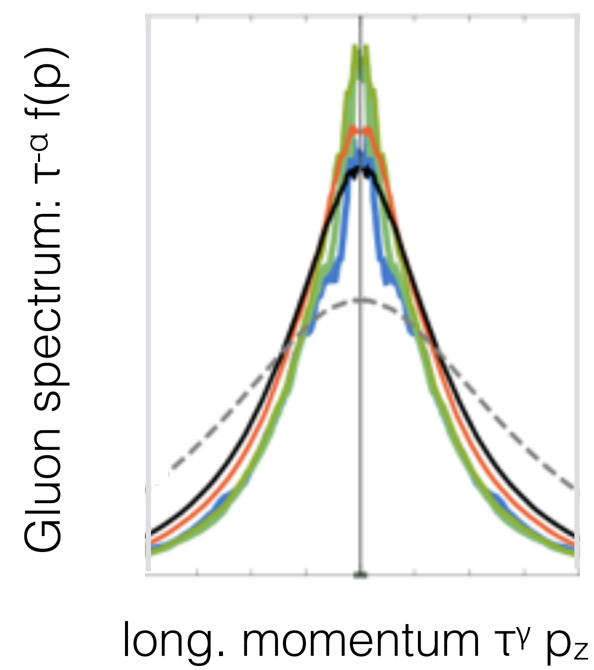

Kurkela, Zhu
PRL 115 (2015) 182301

Classical Yang-Mills

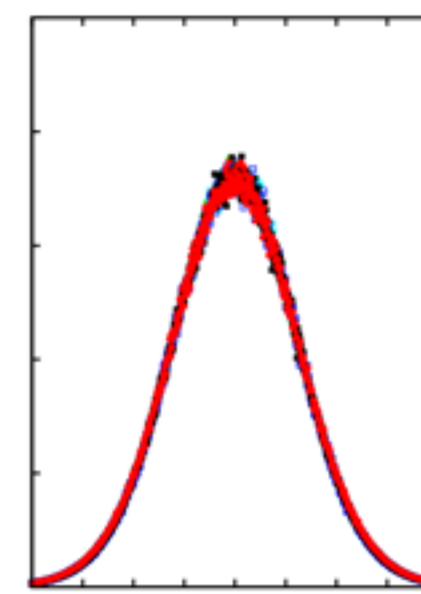

Berges, Boguslavski, SS, Venugopalan
PRD 89 (2014) 074011

-> Effective kinetic description (AMY) can be used to study dynamics of hard modes from $\tau > 1/Q_s$ all the way to equilibration

Bottom-up scenario

Equilibration process beyond $\tau \sim 1/Q_s$ occurs as a three step process
(Baier et al. PLB 502 (2001) 51-58)

Kurkela arXiv:1601.03283

Anisotropy: P_L / P_T

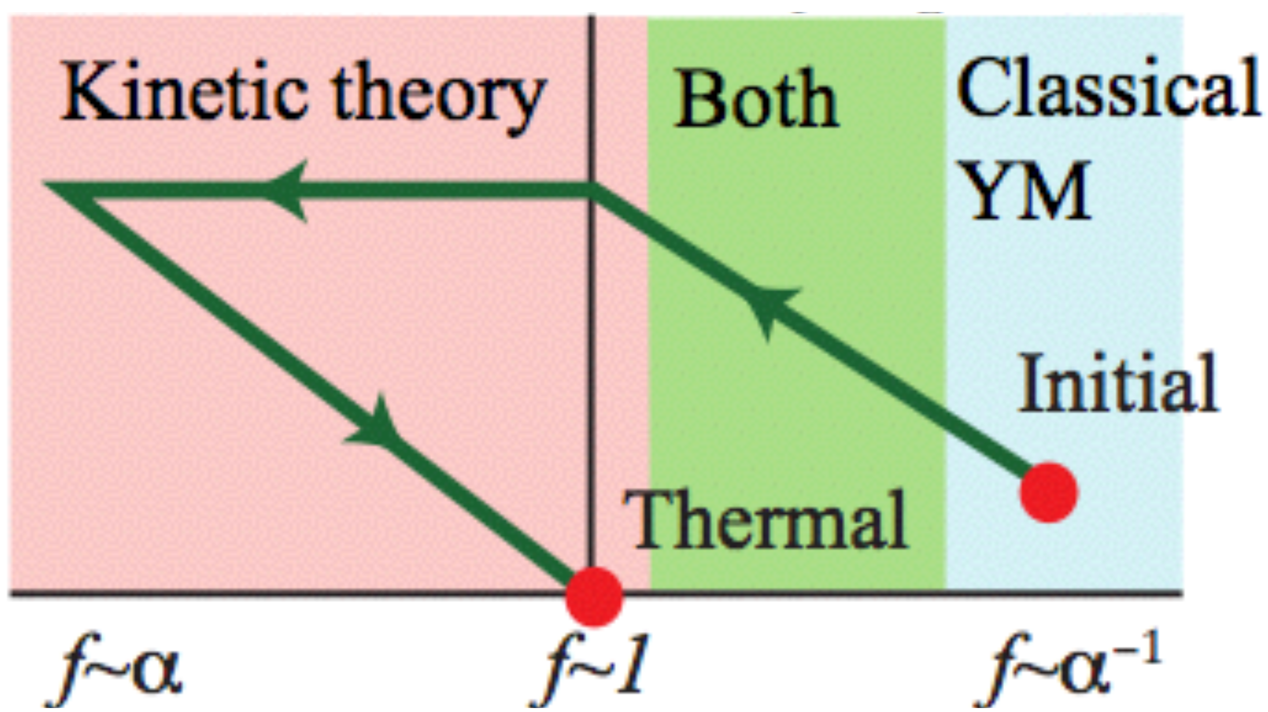

Occupancy: *f*

Berges, Boguslavski, SS, Venugopalan
PRD 89 (2014) 074011

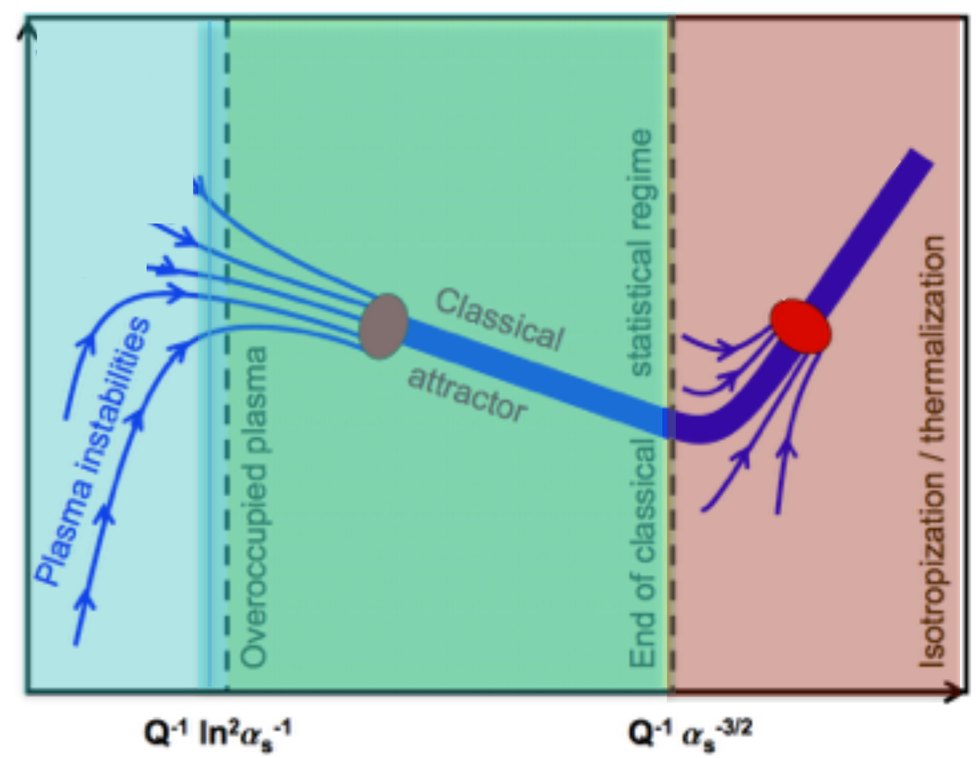

Evolution time: τ

Need to switch from classical Yang-Mills to kinetic description
to describe approach to equilibrium

Quantum regime ($Q_s\tau > \alpha_s^{-3/2}$)

Inelastic processes dominate and lead to a radiative break-up

-> mini-jets loose all their energy to soft thermal bath

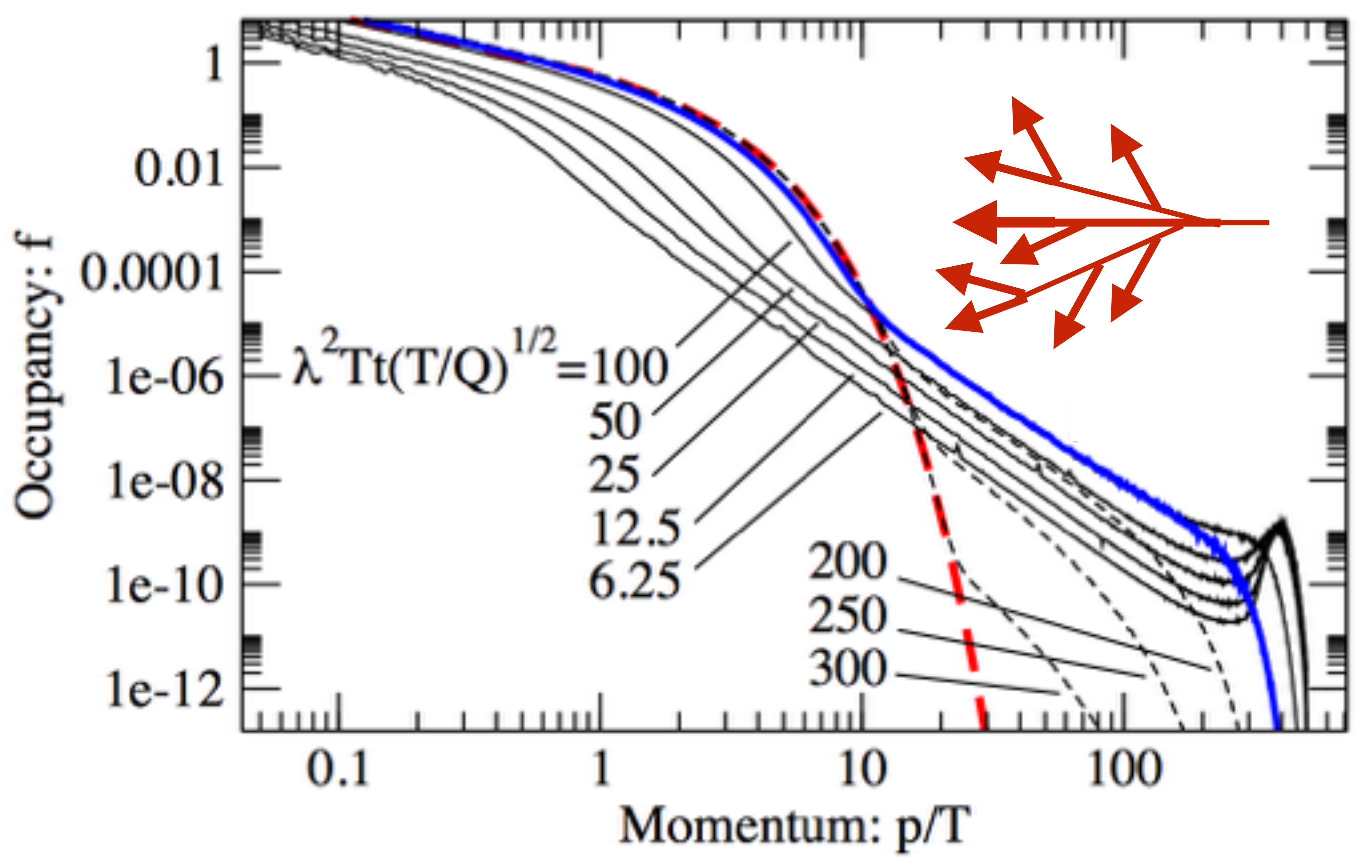

Kurkela, Lu PRL 113 (2014) 182301

equilibration <-> (mini-) jet quenching

Quantum regime ($Q_s\tau > \alpha_s^{-3/2}$)

Inelastic processes dominate and lead to a radiative break-up

-> mini-jets loose all their energy to soft thermal bath

Soft bath heating up due to energy deposited by mini-jets

-> longitudinal pressure rises and system isotropizes

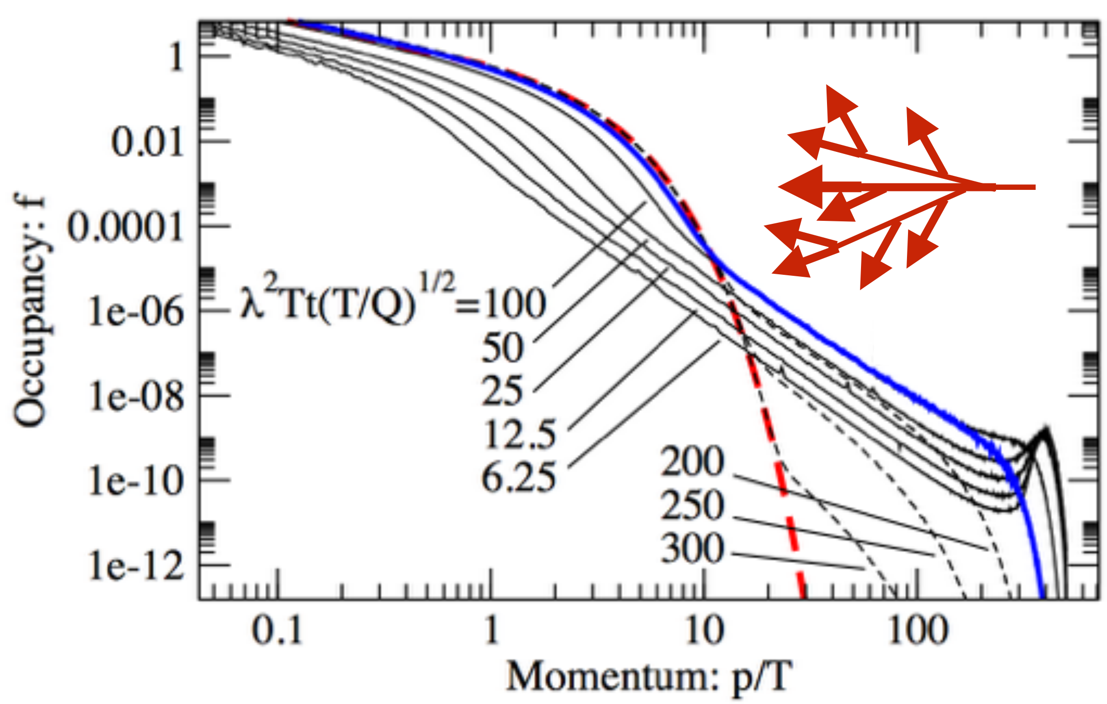

Kurkela, Lu PRL 113 (2014) 182301

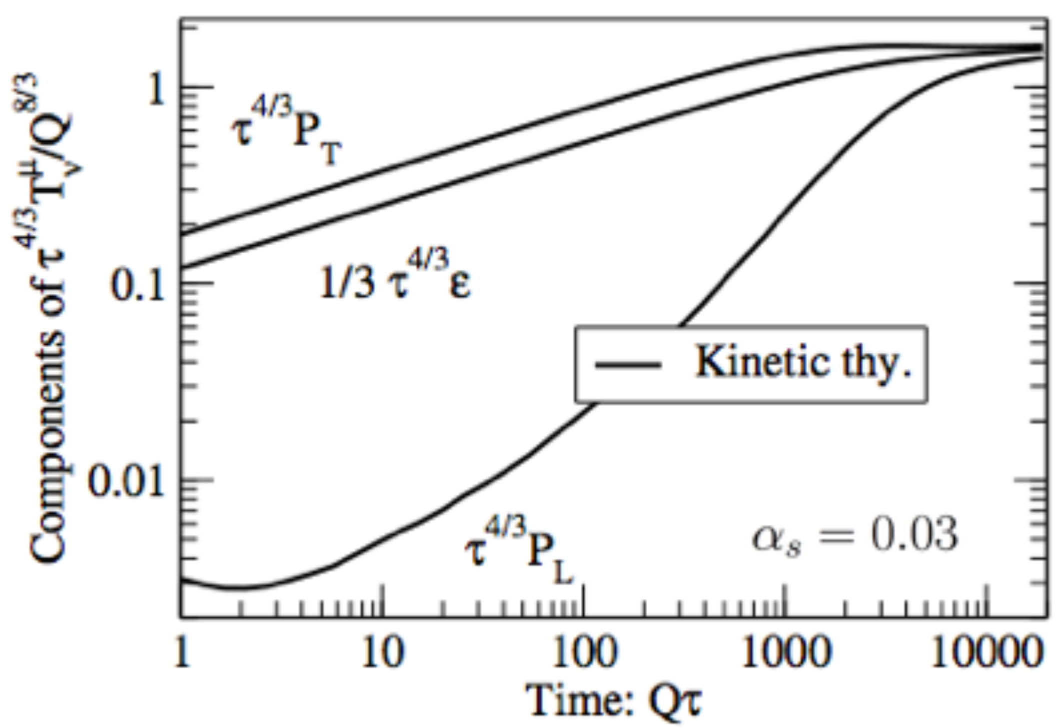

Kurkela, Zhu PRL 115 (2015) 182301

Quantum regime ($Q_s\tau > \alpha_s^{-3/2}$)

Inelastic processes dominate and lead to a radiative break-up

-> mini-jets loose all their energy to soft thermal bath

Soft bath heating up due to energy deposited by mini-jets

-> longitudinal pressure rises and system isotropizes

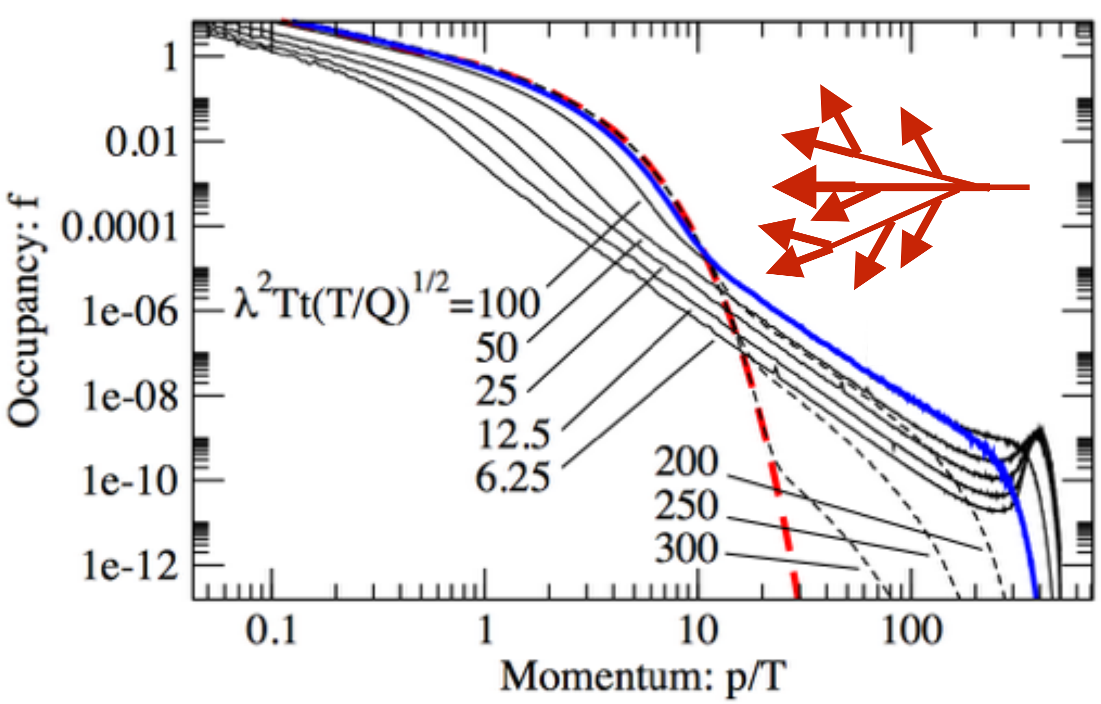

Kurkela, Lu PRL 113 (2014) 182301

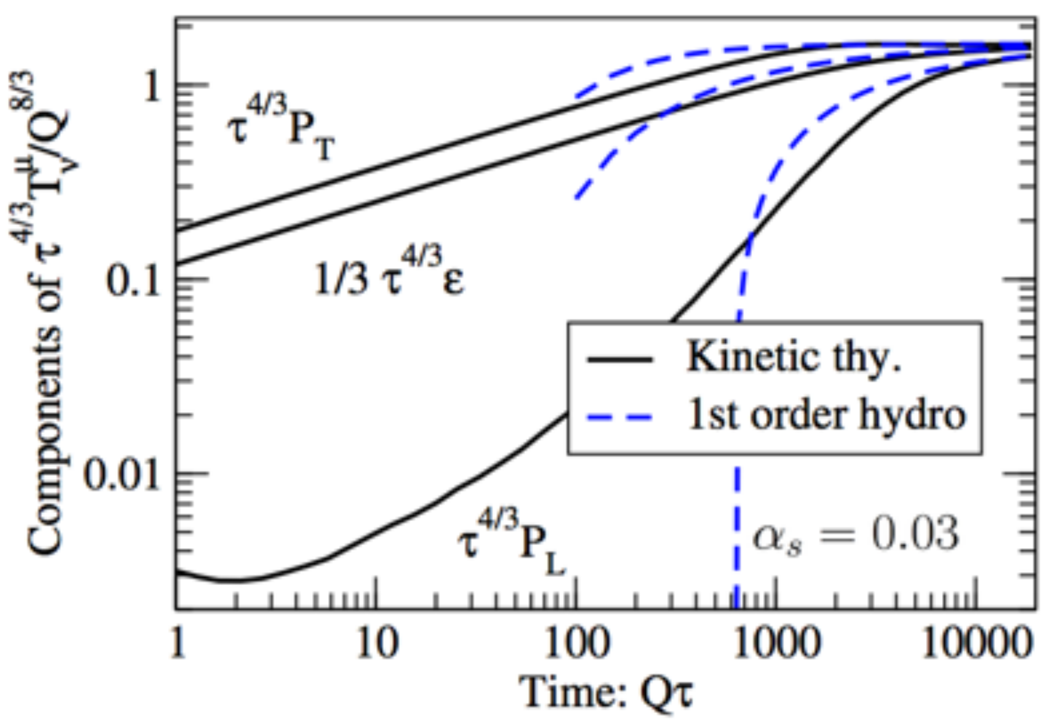

Kurkela, Zhu PRL 115 (2015) 182301

-> smooth matching to hydro-dynamics (no free parameters)

Equilibration process

Clear understanding of the dynamics in the weak-coupling limit

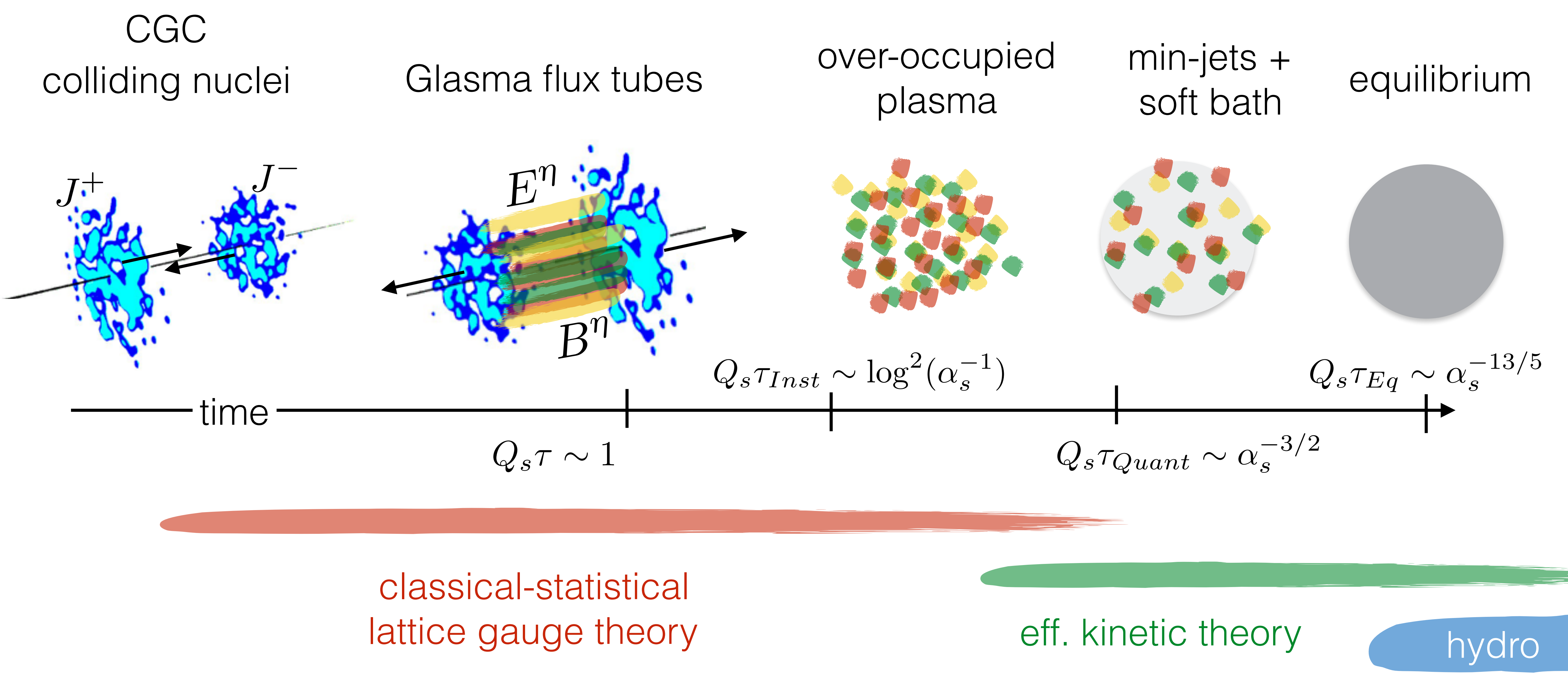

Developed the tools to compute equilibration process from combination of weak-coupling methods

Beyond weak coupling

Extrapolate leading order weak coupling description to physical values α_s=0.3

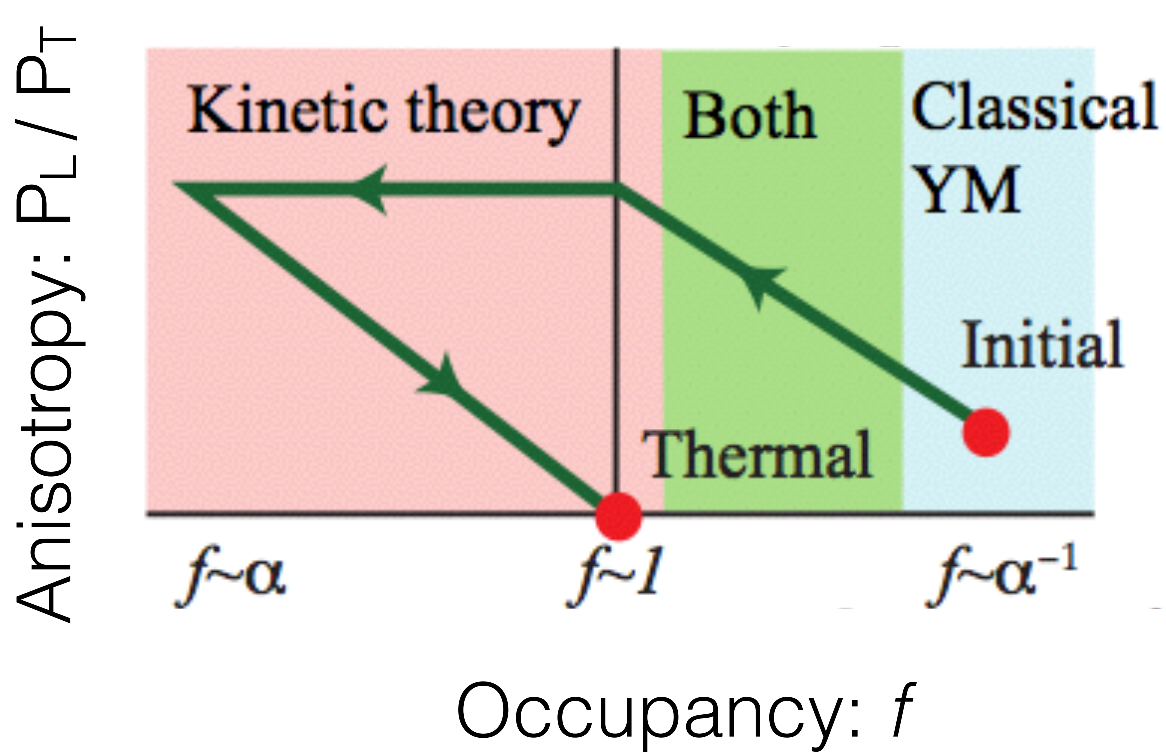

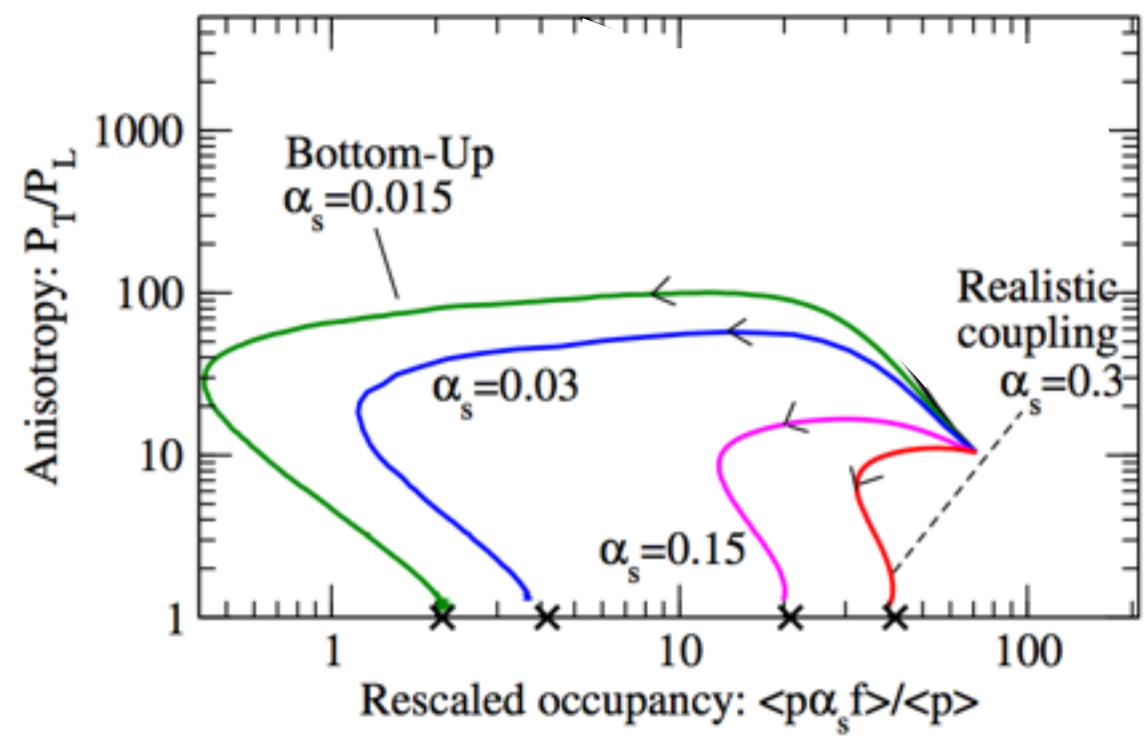

Kurkela, Zhu PRL 115 (2015) 182301

Even though distinctions become less clear
basic mechanism remains the same

Onset of hydrodynamics

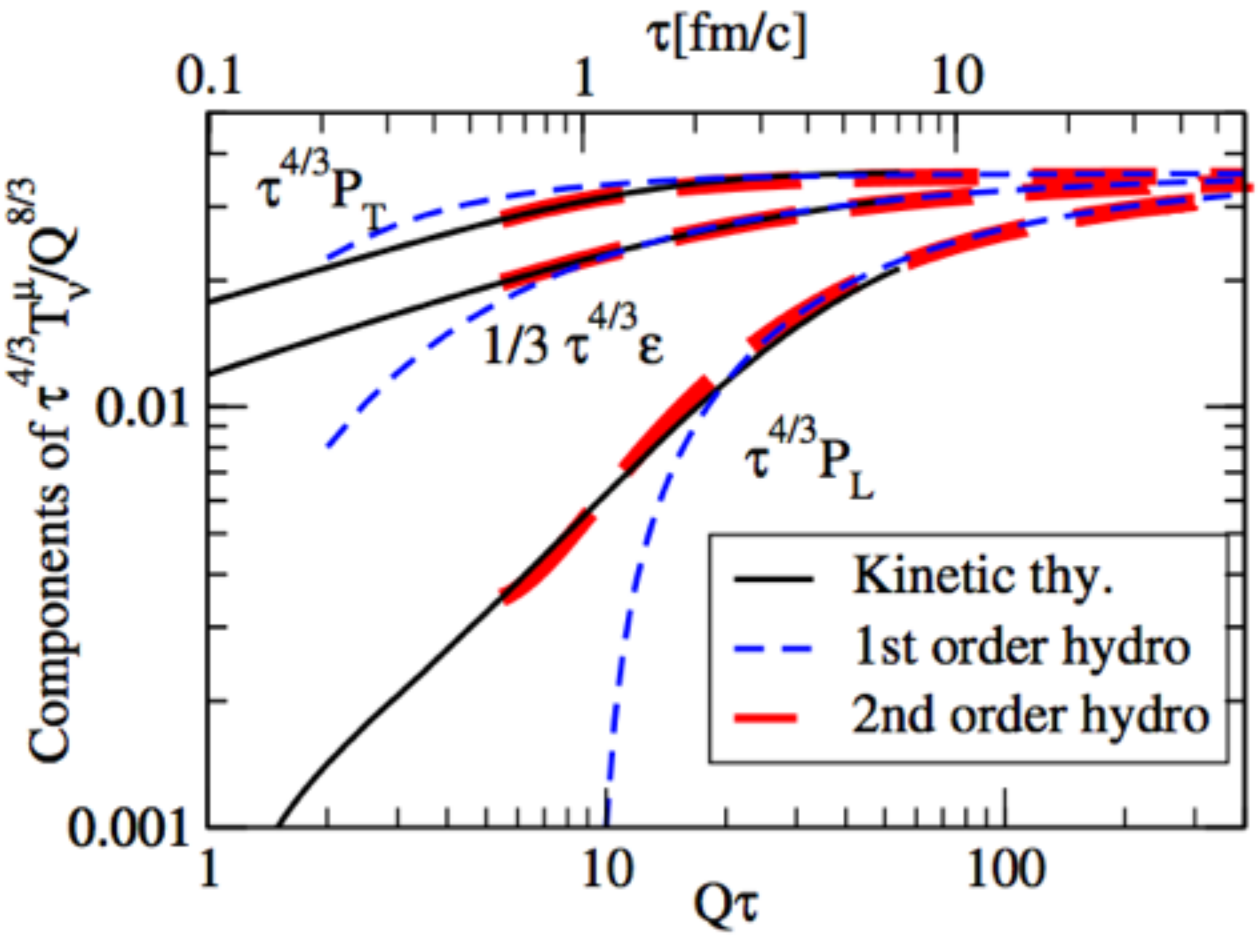

Kurkela, Zhu PRL 115 (2015) 182301

Smooth matching to second order viscous hydrodynamics on a time scale ~1 fm/c

(c.f. talk by Yan Zhu)

Pressure evolution matches for P_L/P_T~1/5

-> Equilibration takes much longer than ~1 fm/c for expanding system

Initial conditions for hydro from weak-coupled equilibrium dynamics

(c.f. talk by Aleksas Mazeliauskas)

String tension

Wilson loops

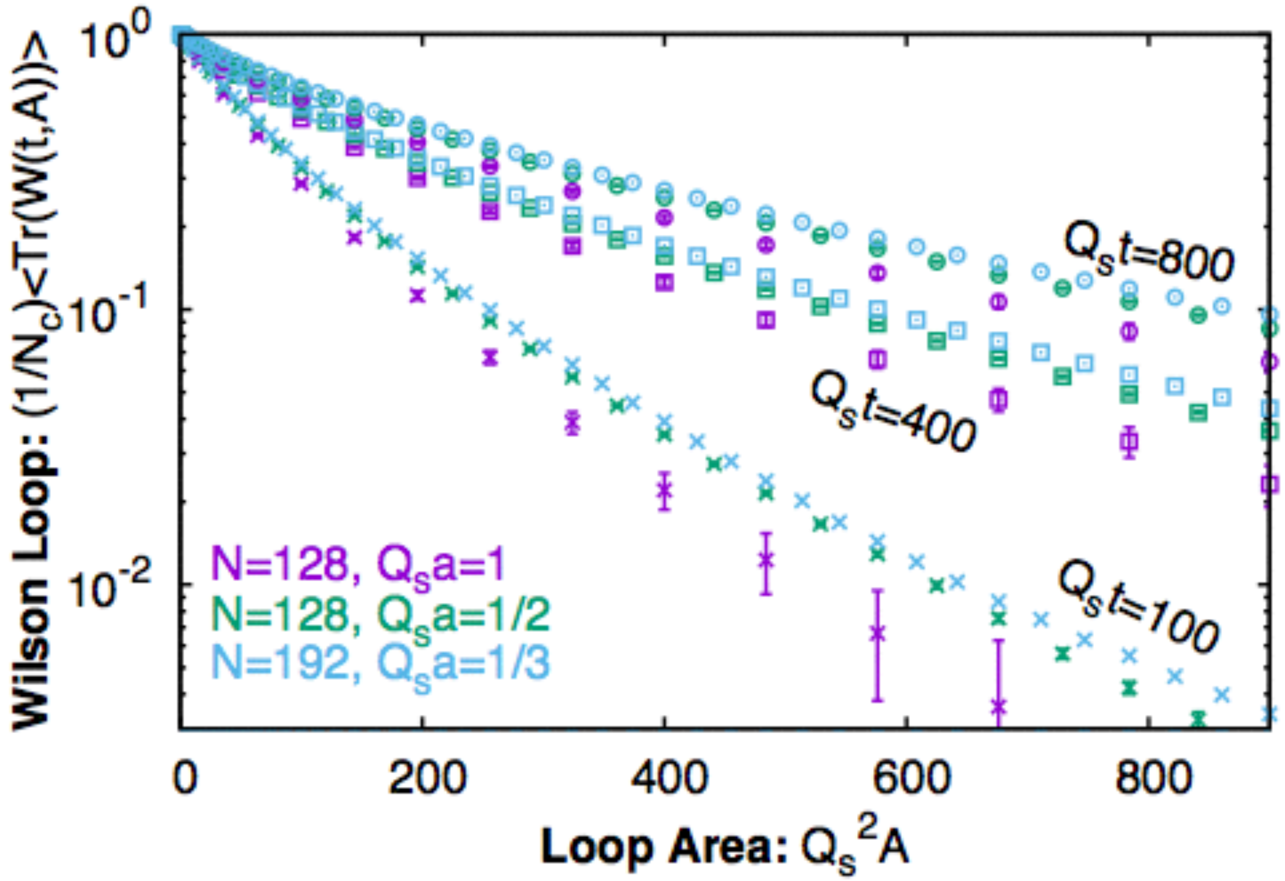

Derivative w.r.t area

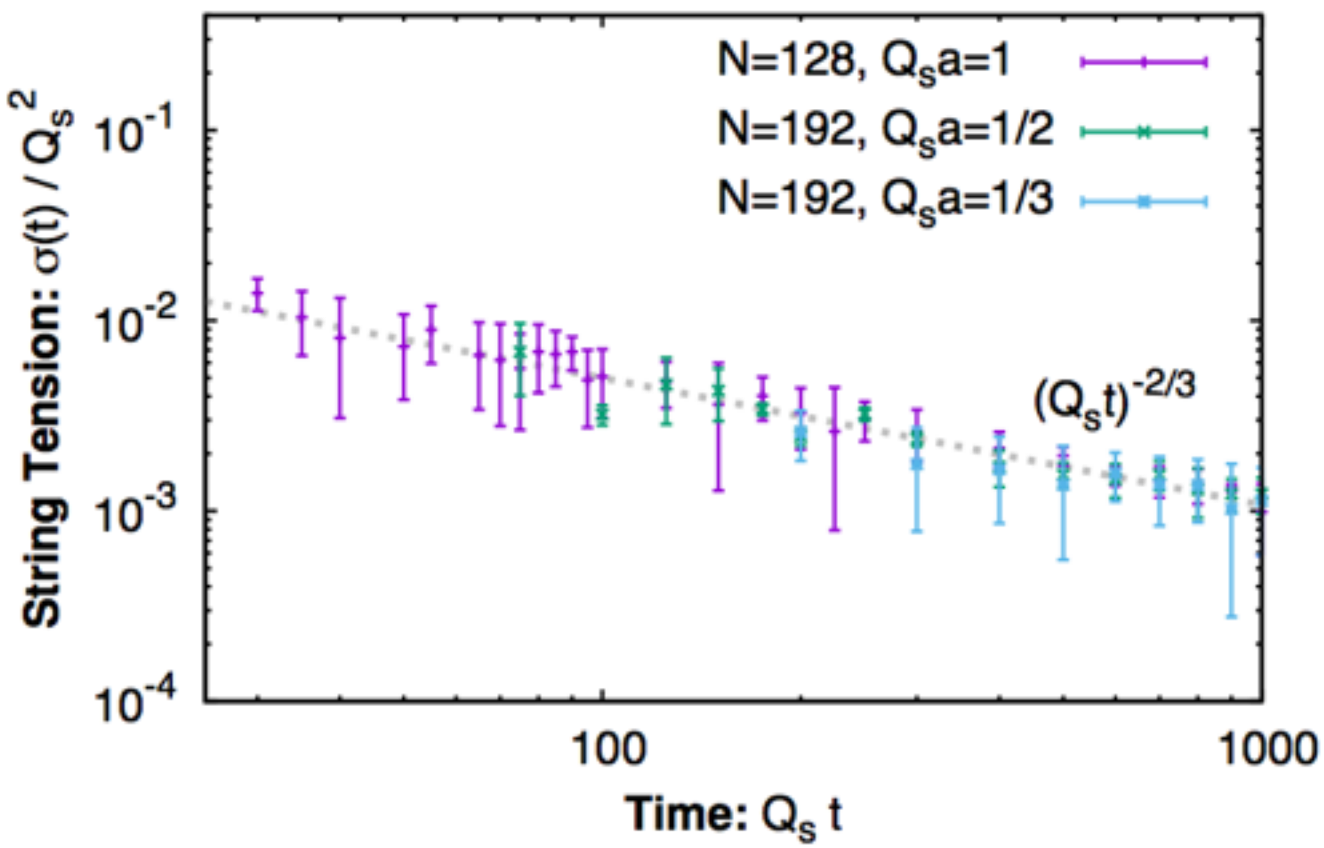

Topology measurement

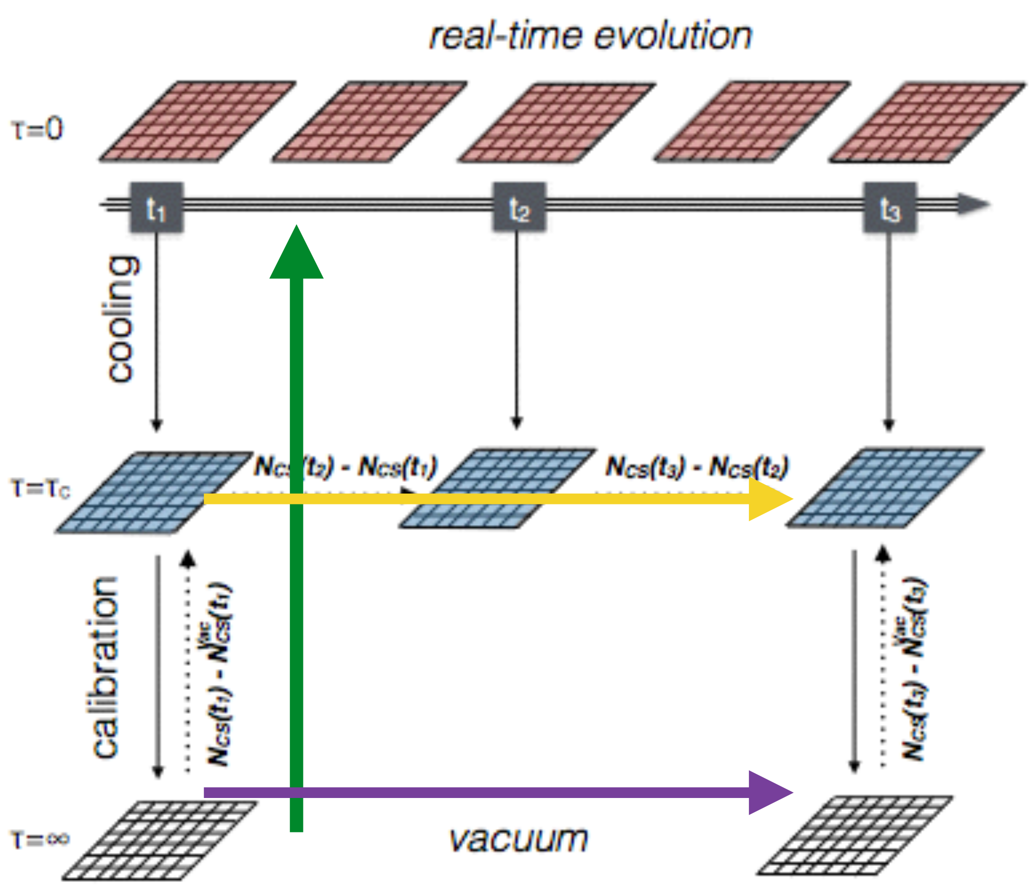

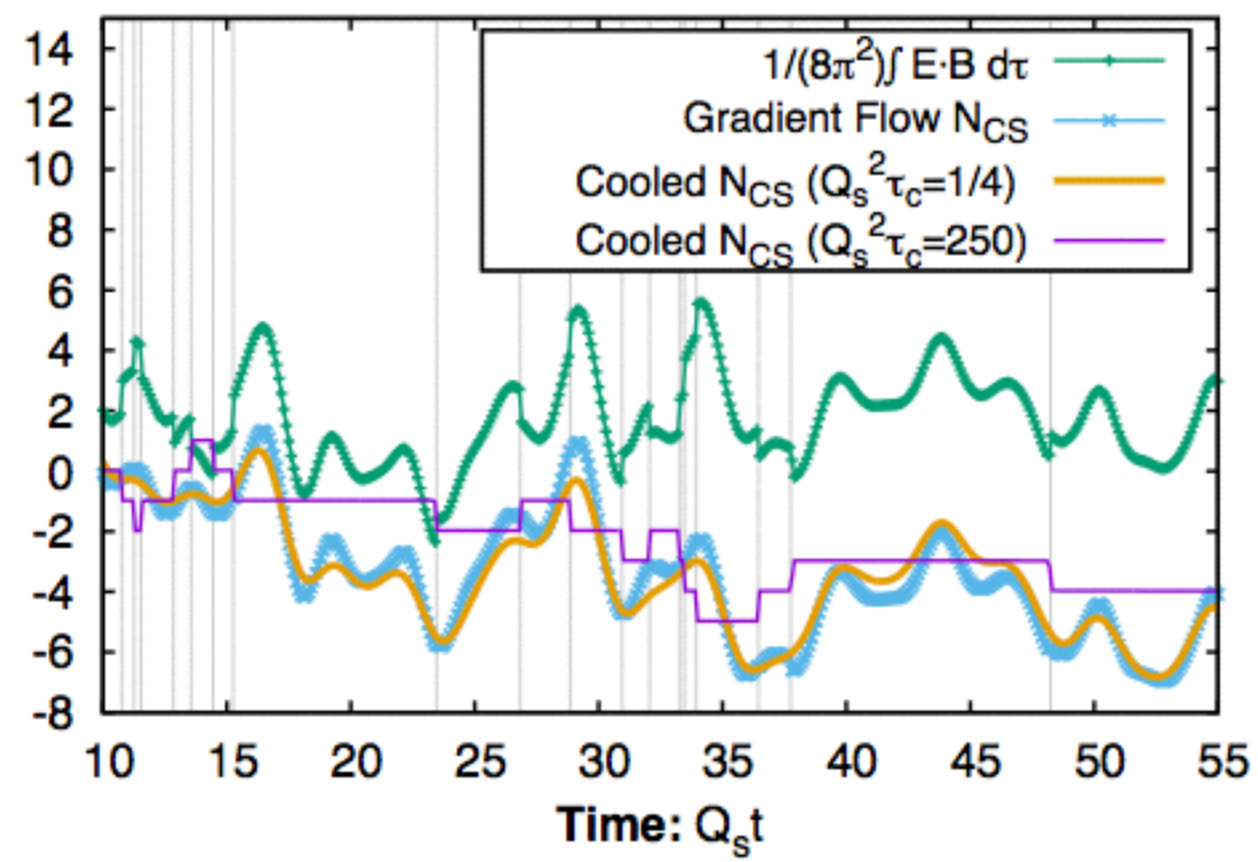

Topology measurement

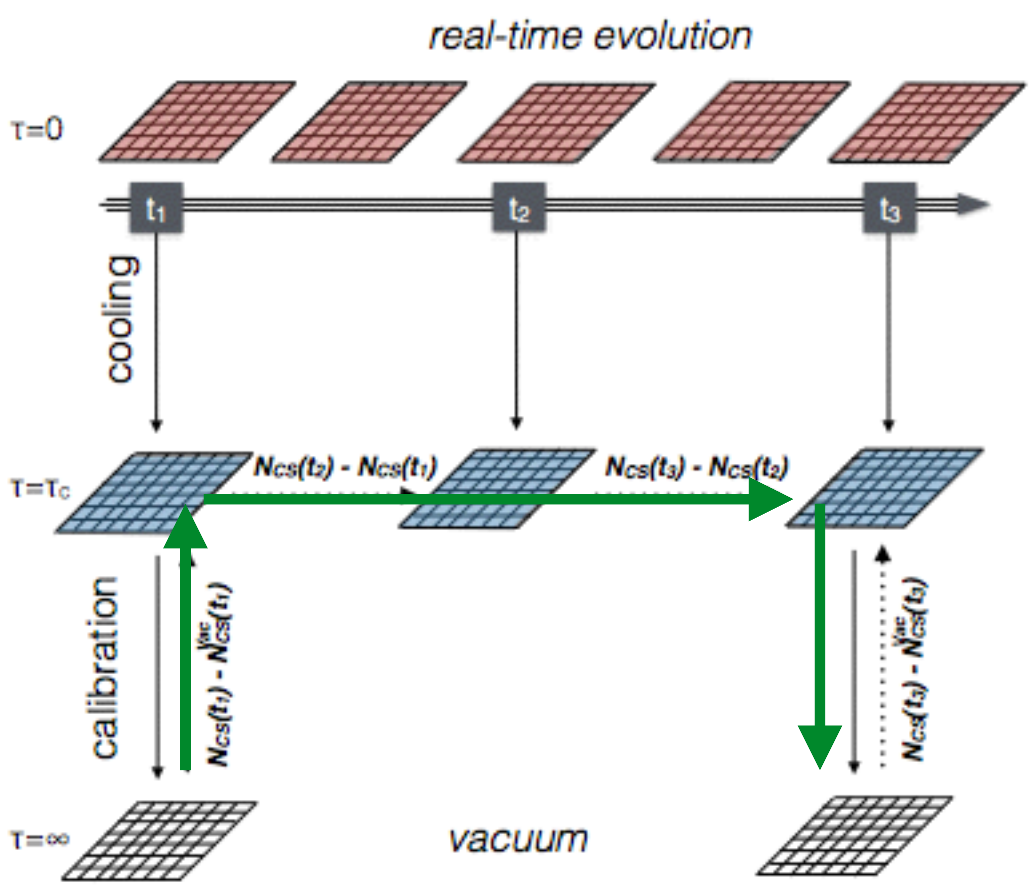

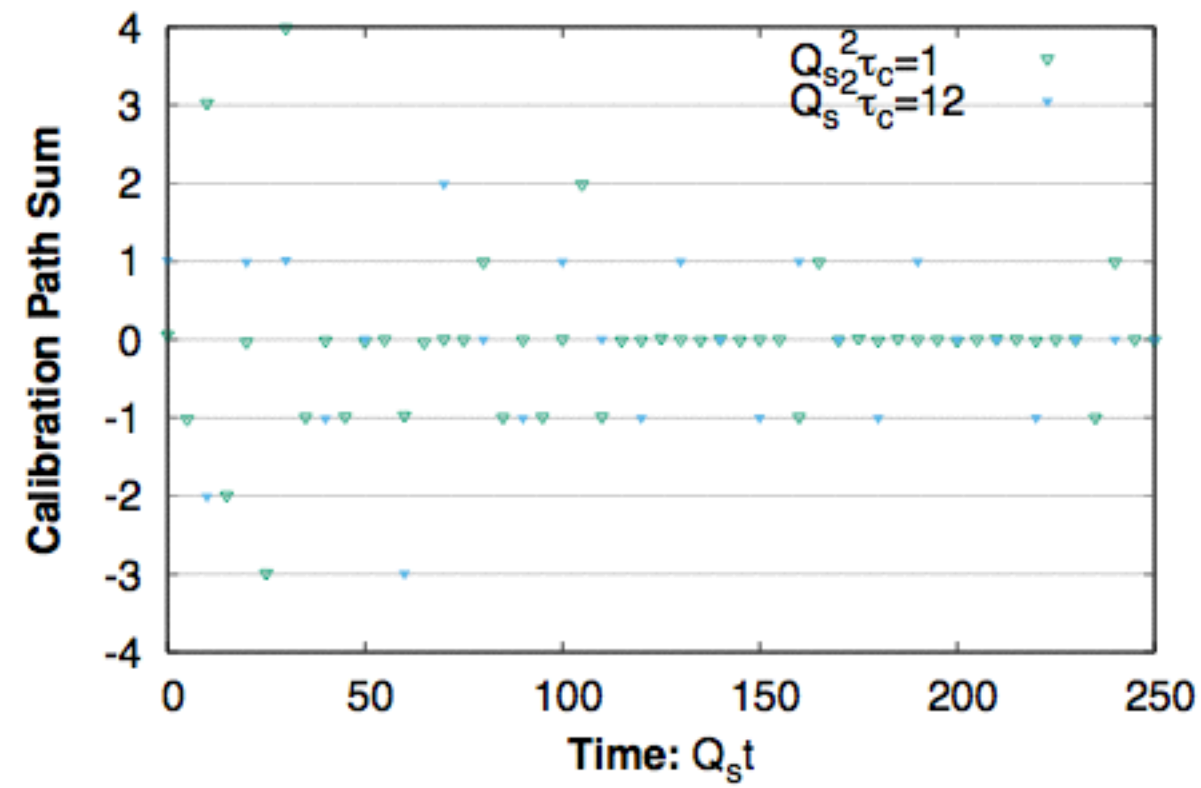

Chern-Simons number Histograms

Generated early (10<Qt<20)

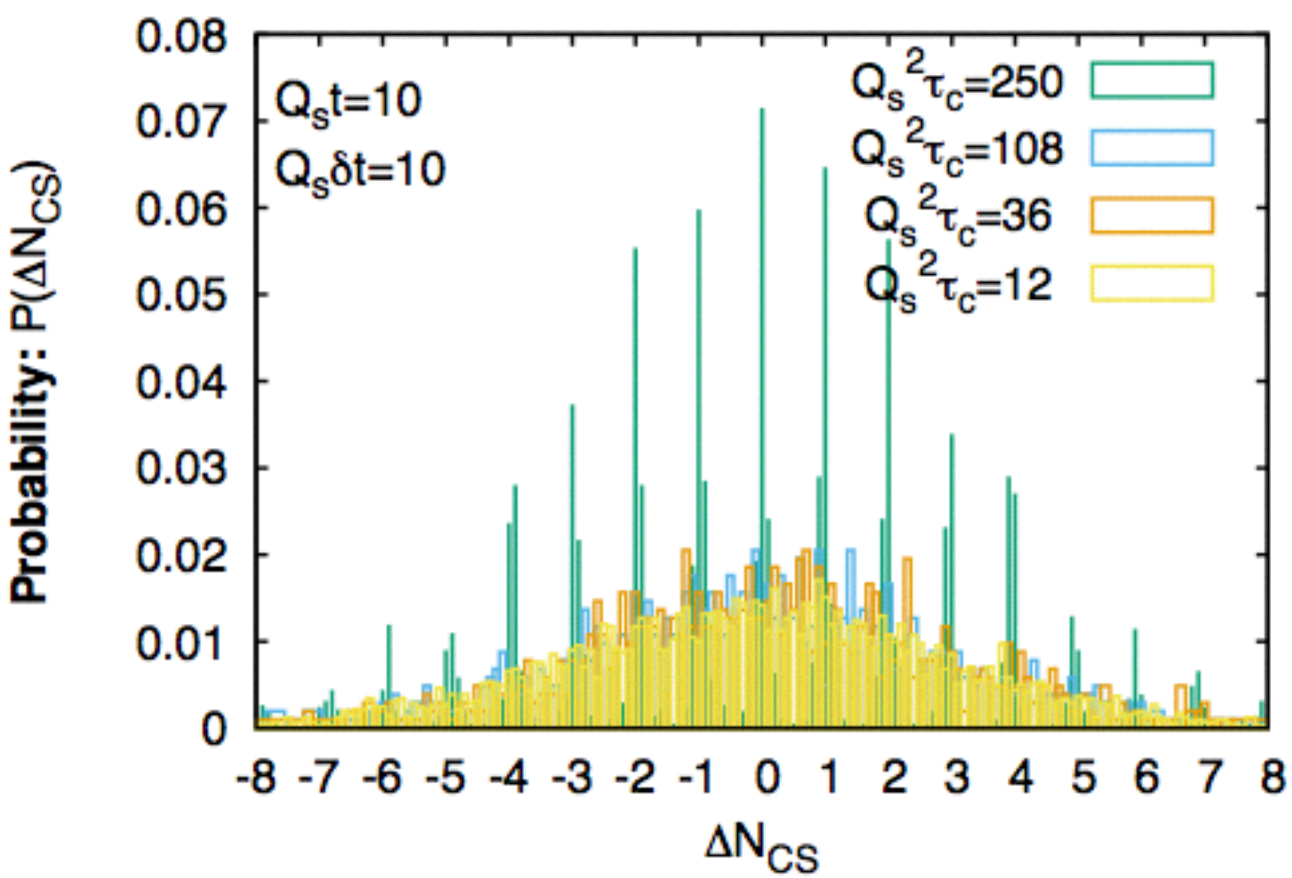

Generated later (50<Qt<60)

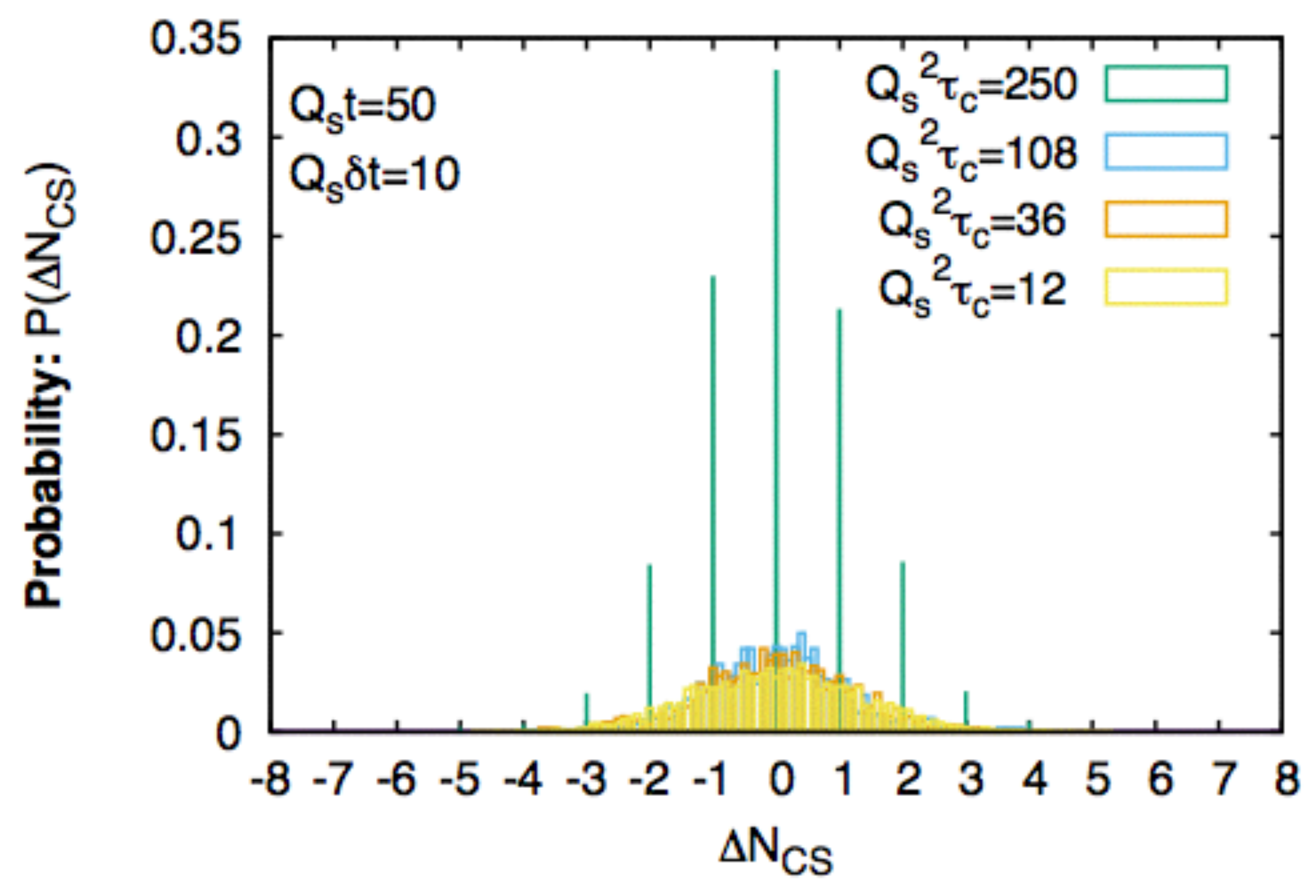

-> Early times dominate generation of axial charge imbalance

Mace, SS, Venugopalan PRD93 (2016) no.7, 074036

Dependence on IC and Cooling depth

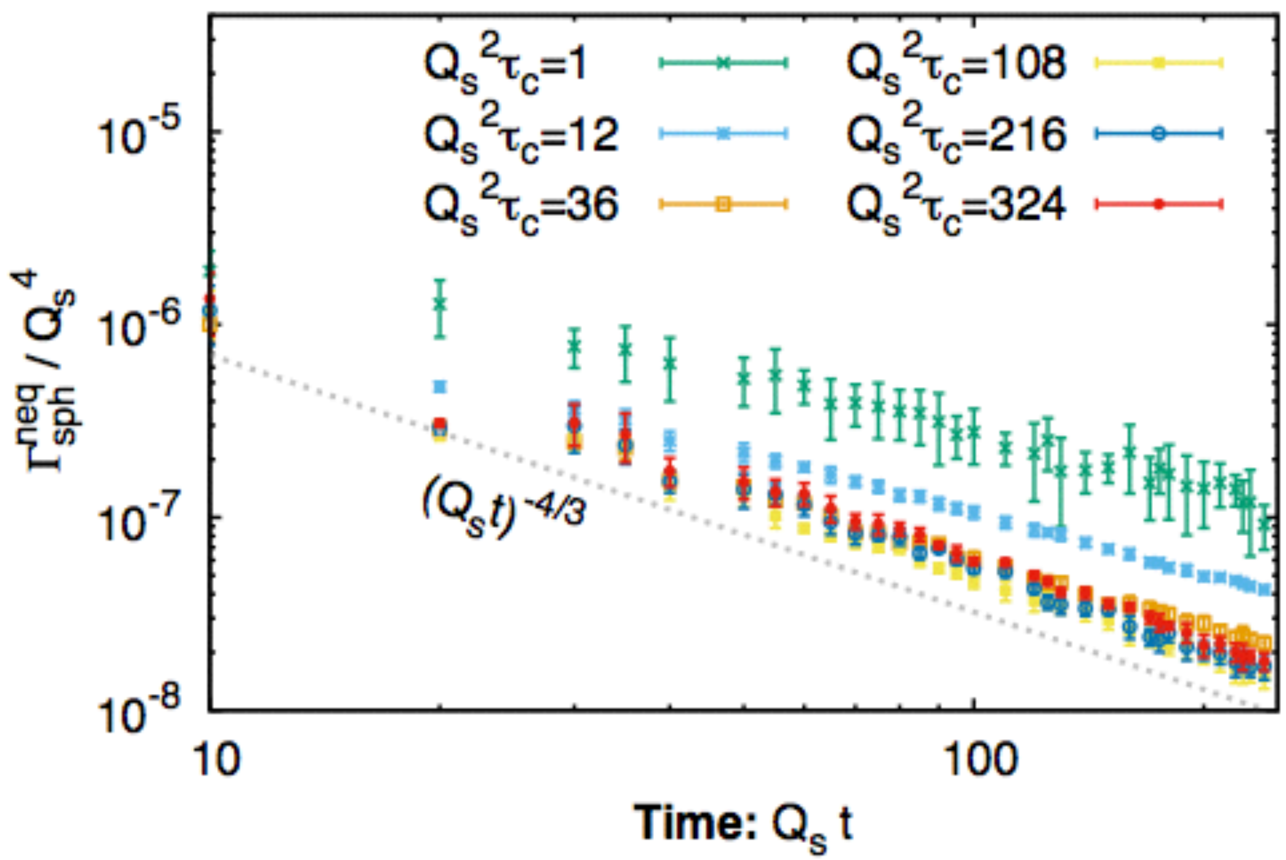

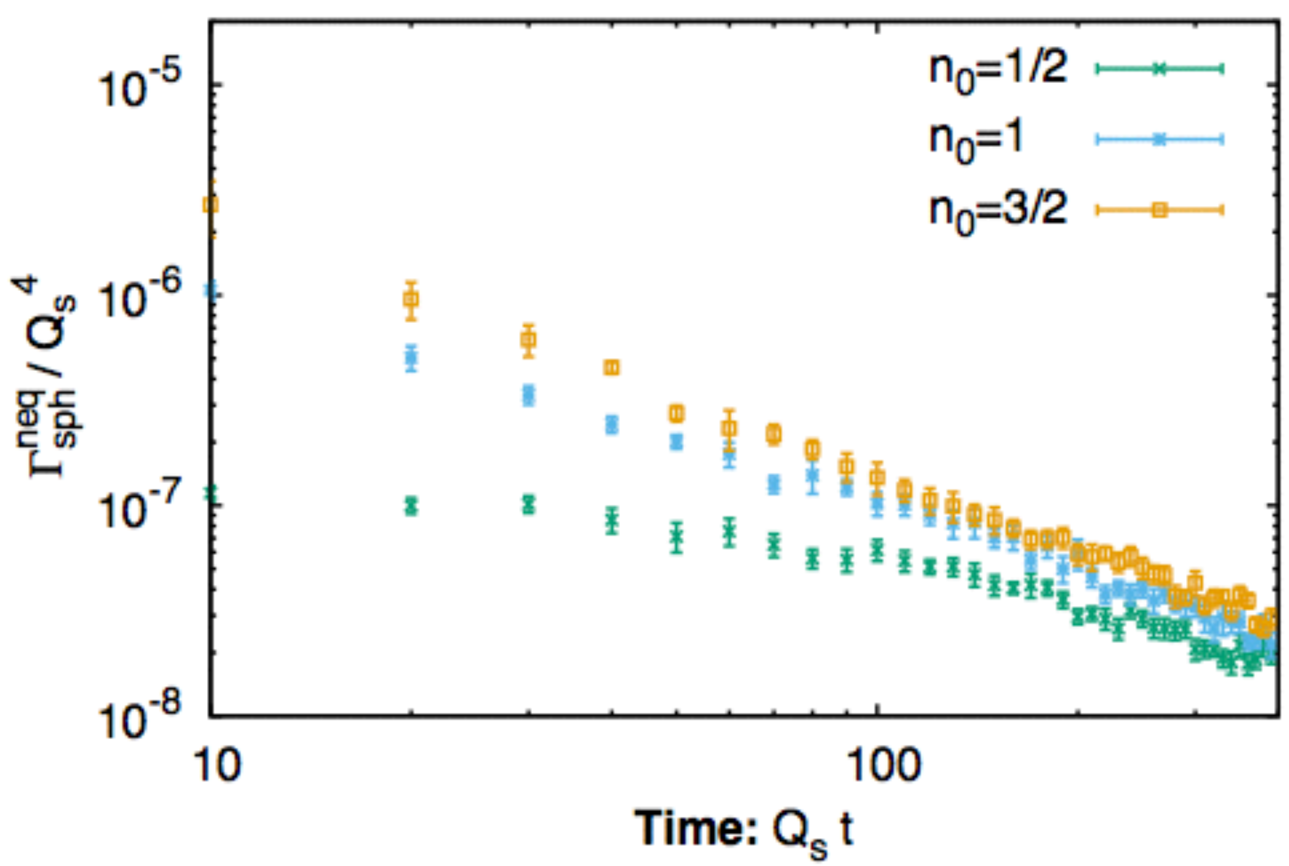

Volume independence